Biochemical Pharmacology 81 (2011) 289–294

Contents lists available at ScienceDirect

Biochemical Pharmacology

journal homepage: www.elsevier.com/locate/biochempharm

Human CYP2A6 is regulated by nuclear factor-erythroid 2 related factor 2

Shin-ichi Yokota, Eriko Higashi, Tatsuki Fukami, Tsuyoshi Yokoi, Miki Nakajima *

Drug Metabolism and Toxicology, Faculty of Pharmaceutical Sciences, Kanazawa University, Kakuma-machi, Kanazawa 920-1192, Japan

ARTICLE INFO

Article history:
Received 27 July 2010
Received in revised form 21 September 2010
Accepted 22 September 2010

Key words:
Cytochrome P450
Nuclear factor-erythroid 2 related factor 2
Transcriptional regulation

ABSTRACT

Human CYP2A6 is responsible for the metabolism of nicotine and coumarin as well as the metabolic activation of tobacco-related nitrosamines. Earlier studies revealed that CYP2A6 activity was increased by dietary cadmium or cruciferous vegetables, but the underlying mechanisms remain to be clarified. In the present study, we investigated the possibility that Nrf2 might be involved in the regulation of CYP2A6. Real-time RT-PCR analysis revealed that the CYP2A6 mRNA level in human hepatocytes was significantly ($P < 0.01$, 1.4-fold) induced by 10 μM sulforaphane (SFN), a typical activator of Nrf2. A computer-based search identified three putative antioxidant response elements (AREs) in the 5′-flanking region of the *CYP2A6* gene at positions −1212, −2444, and −3441, termed ARE1, ARE2, and ARE3, respectively. Electrophoretic mobility shift assays demonstrated that Nrf2 bound only to ARE1. Luciferase assays using HepG2 cells revealed that the overexpression of Nrf2 significantly increased the reporter activities of the constructs containing a 30-bp fragment that included ARE1. However, the activity of the construct containing the intact 5′-flanking region (−1 to −1395) including ARE1 was not increased by the overexpression of Nrf2. In contrast, when the reporter construct was injected into mice via the tail vein, the reporter activity in the liver was significantly ($P < 0.05$, 1.9-fold) increased by SFN (1 mg/head) administration. In conclusion, we found that human CYP2A6 is regulated via Nrf2, suggesting that CYP2A6 is induced under oxidative stress.

© 2010 Elsevier Inc. All rights reserved.

1. Introduction

Human cytochrome P450 2A6 (CYP2A6), which was first purified as coumarin 7-hydroxylase [1], is a major enzyme responsible for the metabolism of nicotine [2] and cotinine [3]. CYP2A6 also metabolically activates tobacco-specific nitrosamines such as 4-methylnitrosoamino-1-(3-pyridyl)-1-butanone and *N*-nitrosonornicotine [4]. Many studies have suggested that the interindividual variability in CYP2A6 activity affects smoking behavior or cancer susceptibility [5–7]. Genetic polymorphisms are the major factor contributing to the interindividual differences in CYP2A6 activity and expression, but dietary or environmental factors as well as endogenous factors such as steroid hormones are also involved. To understand the regulators of CYP2A6 expression, we have studied transcriptional factors regulating CYP2A6 expression and found that pregnane X receptor [8] and estrogen receptor [9] are involved in the CYP2A6 regulation. In addition, a recent study reported the involvement of glucocorticoid receptor in the regulation of CYP2A6 [10].

It has been reported that cadmium ingestion increased the CYP2A6 expression based on the fact that the extent of urinary excretion of cadmium was positively correlated with the extent of urinary excretion of 7-hydroxycoumarin after the administration of coumarin [11]. Mouse Cyp2a5, an orthologue of human CYP2A6, has also been reported to be induced by the administration of cadmium. Abu-Bakar et al. [12] suggested that the induction of Cyp2a5 would be mediated by nuclear factor-erythroid 2 related factor 2 (Nrf2) because the induction was not observed in Nrf2 knock-out mice. Nrf2 is a transcription factor which regulates the expression of antioxidative and cytoprotective genes. Under normal conditions, Nrf2 is sequestered in the cytoplasm by Kelch-like ECH-associated protein 1, which stimulates proteasomal degradation of Nrf2 [13]. On cellular stimulation by oxidative stress, Nrf2 is dissociated from Keap1 and accumulates in the nucleus to regulate the expression of antioxidative and cytoprotective genes. Sulforaphane, which is well known as an activator of Nrf2, is contained in cruciferous vegetables such as broccoli sprouts. Interestingly, it has been reported that CYP2A6 activity was significantly increased after the consumption of broccoli (500 g/day for 6 days) by 1.4- to 5.5-fold [14]. This background prompted us to investigate whether Nrf2 might be involved in the regulation of human CYP2A6.

2. Materials and methods

2.1. Chemicals and reagents

L-Sulforaphane (SFN) and *tert*-butylhydroquinone (tBHQ) were obtained from LKT Laboratory (St. Paul, MN) and Wako Pure

* Corresponding author. Tel.: +81 76 234 4407; fax: +81 76 234 4407.
E-mail address: nmiki@kenroku.kanazawa-u.ac.jp (M. Nakajima).

0006-2952/$ – see front matter © 2010 Elsevier Inc. All rights reserved.
doi:10.1016/j.bcp.2010.09.020

Chemical Industries (Osaka, Japan), respectively. Anti-human Nrf2 antibodies (C-20) and (H-300), which recognize the C-terminus and N-terminus of the Nrf2 protein, respectively, and normal rabbit IgG were purchased from Santa Cruz Biotechnology (Santa Cruz, CA). Dual Luciferase Reporter Assay System, pGL3-basic, phRL-TK, and pGL4.74 plasmid were purchased from Promega (Madison, WI). QIAGEN Plasmid Midi kit was from QIAGEN (Valencia, CA). MiraCLEAN Endotoxin Removal Kit and *Trans*IT-QR Hydrodynamic Delivery Solution were from Mirus Bio (Madison, WI). Oligonucleotides were commercially synthesized at Hokkaido System Sciences (Sapporo, Japan). Restriction enzymes were purchased from Takara (Shiga, Japan), TOYOBO (Osaka, Japan), and New England Biolabs (Beverly, MA). All other reagents were of the highest grade commercially available.

2.2. Cell culture

Human cryopreserved hepatocytes, lot 82 (Hispanic, female, 23 years) were purchased from In Vitro Technologies (Baltimore, MD). The hepatocytes were seeded into collagen-coated 6-well plates at 0.9×10^5 cells/well and maintained in HCM hepatocyte culture medium (Cambrex, East Rutherford, NJ) at 37 °C under 5% CO_2. After 24 h, the culture medium was changed to HCM medium (epidermal growth factor- and antibiotics-free) containing 10 μM SFN or 0.1% (v/v) DMSO vehicle. Hepatocytes were maintained for 12 h or 24 h until harvesting.

Human hepatoma cell line HepG2 was obtained from American Type Culture Collection (Manassas, VA). HepG2 cells were cultured in Dulbecco's modified Eagle's medium (DMEM) (Nissui Pharmaceutical, Tokyo, Japan) supplemented with 10% fetal bovine serum (FBS) (Invitrogen, Carlsbad, CA) and 0.1 mM nonessential amino acids (Invitrogen) at 37 °C under 5% CO_2.

2.3. Real-time RT-PCR analyses

Total RNA was isolated from human hepatocytes or mouse liver using RNAiso (Takara) following the manufacturer's protocol, and cDNA was synthesized as described previously [15]. The primers for human CYP2A6 [15] and human GAPDH [16] were described previously. The forward and reverse primers for mouse NAD(P)H:-quinone oxidoreductase 1 (NQO1) were 5′-CCCTGATTGTACTGGCC-CATT-3′ and 5′-CGTCCTTCCTTATATGCTAG-3′, respectively. The forward and reverse primers for mouse GAPDH were 5′-AAATGGGGTGAGGCCGGT-3′ and 5′-ATTGCTGACAATCTTGAGTGA-3′, respectively. Real-time RT-PCR assays were performed using the Smart Cycler (Cepheid, Sunnyvale, CA) as described previously [17].

2.4. Electrophoretic mobility shift assays

Double-stranded oligonucleotides were labeled with [γ-^{32}P] ATP using T4 polynucleotide kinase (TOYOBO) and purified by Microspin G-50 columns (GE Healthcare, Buckinghamshire, UK). The oligonucleotide sequences for ARE1 and consensus ARE (cARE) on *Mus musculus* heme oxygenase-1 (HO-1) promoter were 5′-GTAG-TAGCCCCTGACAAAGCAGGAATCAT-3′ and 5′-GATCTTTTATGCT-GAGTCATGGTTT-3′, respectively [18]. The labeled probe (80 fmol, ~13,000 cpm) was applied to each binding reaction in 25 mM HEPES-KOH (pH 7.9), 0.5 mM EDTA, 10% glycerol, 50 mM KCl, 0.5 mM dithiothreitol, 0.5 mM (*p*-amidinophenyl) methanesulfonyl fluoride, 1 μg of poly (dI-dC), 10 μg of salmon sperm DNA, and 8 μg of the nuclear extracts from 80 μM tBHQ-treated HepG2 cells with a final reaction volume of 15 μl. To determine the specificity of the binding to the oligonucleotides, competition experiments were conducted by co-incubation with 10-, 50-, and 200-fold excesses of unlabeled competitors. For super-shift experiments, 2 μg of anti-Nrf2 antibodies or normal rabbit IgG were pre-incubated with the nuclear protein on ice for 30 min. The reactions were incubated on ice for 15 min and then loaded on 4% acrylamide gel in 0.5 × Tris-borate EDTA buffer. The gels were dried and exposed to imaging plate for 18 h. The DNA-protein complexes were detected with a Fuji Bio-Imaging Analyzer BAS 1000 (Fuji Film, Tokyo, Japan).

2.5. Human Nrf2 expression plasmid and reporter constructs

Human Nrf2 expression plasmid and the pGL3-cARE plasmid containing two copies of the cARE on the human *NQO-1* gene were previously constructed [17]. Double-stranded oligonucleotide ARE1 on the human *CYP2A6* gene (5′-GTAGTAGCCCCTGA-CAAAGCAGGAATCAT-3′) was cloned into the pGL3-tk plasmid digested with *Sma* I, resulting in single (pGL3/ARE1) and double (pGL3/2 × ARE1) insertions. The pGL3/-3046 plasmid containing the 5′-flanking region from −3046 to −1 of the *CYP2A6* gene was previously constructed [9]. The pGL3/−1395 and pGL3/−185 plasmids were constructed by ligating the fragments from pGL3/−3046 plasmid digested with *BST1107* I/*Hind* III and *Pvu* II/*Hind* III, respectively, into the *Sma* I/*Hind* III-digested pGL3-basic plasmid. The pGL3/−1013 plasmid was constructed by ligating the fragments from pGL3/−3046 plasmid digested with *Bgl* II/*Hind* III into the *Bgl* II/*Hind* III-digested pGL3-basic plasmid. The plasmid DNA was purified by QIAGEN Plasmid Midi kit (QIAGEN). Nucleotide sequences of the constructed plasmids were confirmed by DNA sequencing analyses.

2.6. In vitro transfection and luciferase assay

HepG2 cells were seeded into 24-well plates at 1.0×10^5 cells/well and incubated for 24 h before transfection. Transfection was performed using Tfx-20 reagent (Promega). In brief, the transfection mixture consisted of 150 ng of pGL3 plasmids, 5 ng of phRL-TK plasmid, and 100 ng of Nrf2 expression plasmid (or control vector). Forty-eight hours after the transfection, the cells were harvested and lysed to measure the luciferase activity using a Dual Luciferase Reporter Assay System. The relative luciferase activities were normalized with the *Renilla* luciferase activities.

2.7. In vivo transfection

Male ICR mice (3 weeks old, 10–13 g) were obtained from SLC Japan (Hamamatsu, Japan). Mice were housed in a controlled environment (temperature 25 ± 1 °C, humidity 50 ± 10%, and 12 h light/12 h dark cycle) in the institutional animal facility with access to food and water *ad libitum*. Mice were acclimatized for a week before use for the experiments. For in vivo transfection, 18–22 g mice were injected via the tail vein with 10 μg of pGL3 plasmids and 1 μg of pGL4.74 plasmid, in volumes of 0.1 ml/g of body weight within 5–8 s using the *Trans*IT-QR Hydrodynamic Delivery Solution. Endotoxin in plasmid preparations was removed using MiraCLEAN Endotoxin Removal Kit. After 18 h, 1 mg/head SFN or saline was intraperitoneally administered. The dose was decided referring previous studies [19,20]. Animals were sacrificed 24 h later and the liver, approximately 100 mg, was removed and homogenized in 1 ml of passive lysis buffer (Dual Luciferase Reporter Assay System). The liver homogenates were centrifuged at 15,000 rpm for 10 min at 4 °C. Twenty microliters of the supernatant were used to measure the firefly and *Renilla* luciferase activities. For each construct, at least three mice were transfected, and three independent experiments were performed. Animal maintenance and treatment were conducted in accordance with the National Institutes of Health Guide for Animal Welfare of Japan, as approved by the Institutional Animal Care and Use Committee of Kanazawa University, Japan.

2.8. Statistical analysis

Data are expressed as mean ± SD. Statistical analysis was performed by an unpaired two-tailed Student's *t* test. A value of *P* less than 0.05 was considered statistically significant.

3. Results

3.1. SFN induces CYP2A6 mRNA expression in human hepatocytes

We first examined whether the CYP2A6 level in human hepatocytes was increased by SFN treatment (Fig. 1). When human hepatocytes were treated with 10 μM SFN for 12 h, a significant induction (1.4-fold, $P < 0.01$) of the CYP2A6 mRNA level was observed. With 24-h treatment, a similar induction (1.3-fold induction, $P < 0.05$) was observed. These results suggest that CYP2A6 mRNA is induced by SFN.

3.2. Nrf2 directly binds to the ARE on the CYP2A6 gene

To find potential binding sites of Nrf2 on the 5′-flanking region of *CYP2A6* gene, we investigated overlapping with the core sequence of consensus ARE 5′-TMAnnRTGAY(C/T)nnnGCRwwww-3′ (core sequence is underlined) using a computer program GENETYX-MAC for all probable nucleotide combination, and thereby we identified three putative AREs up to −4 kb of the 5′-flanking region of *CYP2A6* gene. These elements located at −1212, −2444, and −3441 were termed ARE1, ARE2, and ARE3, respectively (Fig. 2). We performed electrophoretic mobility shift assays to examine whether Nrf2 can bind to these AREs (Fig. 3). When the ^{32}P-labeled cARE was incubated with the nuclear extract prepared from the tBHQ-treated HepG2 cells, three bands were detected (Fig. 3, lane 1). The upper and lower bands were non-specific bands (NS). The middle band represented a shifted band, and its density was diminished with both anti-Nrf2 antibodies (C-20) and (H-300) (Fig. 3, lanes 2 and 3).

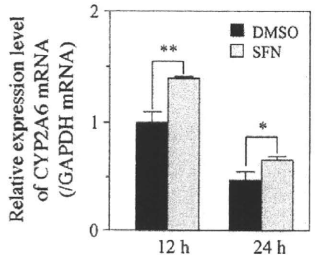

Fig. 1. Effects of SFN treatment on the CYP2A6 mRNA level in human hepatocytes. Human hepatocytes were treated with 10 μM SFN or 0.1% DMSO for 12 h or 24 h. Total RNA was extracted and real-time RT-PCR was performed. To normalize the RNA loading, the CYP2A6 mRNA levels were corrected with the GAPDH mRNA levels. Each column represents the mean ± SD of three independent experiments. *$P < 0.05$ and **$P < 0.01$ compared with DMSO treatment.

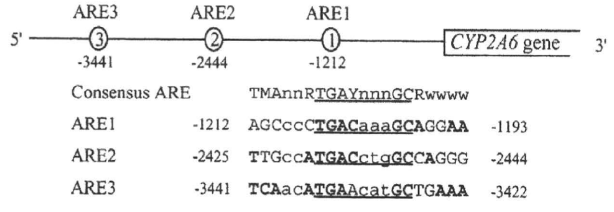

Fig. 2. Schematic representation of the putative AREs on the *CYP2A6* genes and the sequences of the AREs. Numbers indicate the nucleotide position when the A in the initiation codon ATG is denoted +1 and the base before A is numbered −1. The core ARE sequence is underlined. The nucleotides that are consistent with the consensus ARE are shown with bold letters.

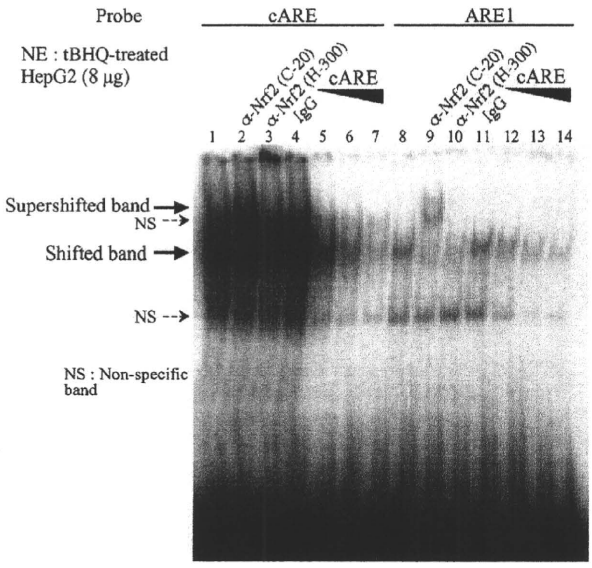

Fig. 3. Electrophoretic mobility shift assays of the binding of Nrf2 to ARE of the *CYP2A6* gene. Oligonucleotides of the cARE in *Mus musculus* HO-1 promoter (*left*) and CYP2A6 ARE1 (*right*) were used as probes. Nuclear extracts were prepared from HepG2 cells treated with 80 μM tBHQ for 6 h. Cold oligonucleotides were used as a competitor in 10-, 50-, and 200-fold molar excess. For supershift analyses, 2 μg of anti-Nrf2 antibodies or normal rabbit IgG were preincubated with the nuclear extracts on ice for 30 min.

Super-shifted band was observed only with the anti-Nrf2 antibody (C-20), consistent with our previous study on UGT2B7 [17]. When the ARE1 was used as a probe, a band the mobility of which was the same as that of the cARE–Nrf2 complex was observed (Fig. 3, lane 8). The band was clearly supershifted with the anti-Nrf2 antibody (C-20) (Fig. 3, lane 9) and was competed out by unlabeled cARE (Fig. 3, lanes 12–14). These results indicated that Nrf2 specifically binds to ARE1 on the human *CYP2A6* gene. When ARE2 or ARE3 was used as a probe, no band was observed (data not shown).

3.3. ARE1 on CYP2A6 promoter is functional for transactivation via Nrf2

To examine whether ARE1 is functional for the transactivation via Nrf2, luciferase assays were performed using HepG2 cells. We first confirmed that the luciferase activity of the pGL3-cARE plasmid containing two copies of cARE used as a positive control, was significantly ($P < 0.001$) increased up to 2.7-fold by the overexpression of Nrf2 (Fig. 4A). The luciferase activities of the pGL3/ARE1 and pGL3/2 × ARE1 plasmids containing one and two copies of ARE1 were significantly increased up to 1.3- and 2.0-fold, respectively, by the overexpression of Nrf2. Next we performed luciferase assay using a series of reporter plasmids containing the 5′-flanking region of *CYP2A6* gene (Fig. 4B). Contrary to our expectations, the luciferase activity of the pGL3/−1013 plasmid containing ARE1 was significantly decreased by the overexpression of Nrf2. The luciferase activities of the pGL3/−1395 and pGL3/−185 plasmids were also significantly decreased by the overexpression of Nrf2. These results suggest that the proximal promoter region possibly has a negative regulatory region responding to Nrf2, or HepG2 cells may lack transcriptional factors crucial for the transcriptional activity of CYP2A6.

3.4. Nrf2 activates CYP2A6 promoter activity in vivo

Next, we sought to determine the transactivity of the plasmids in mice in vivo, because mice liver contains sufficient levels of

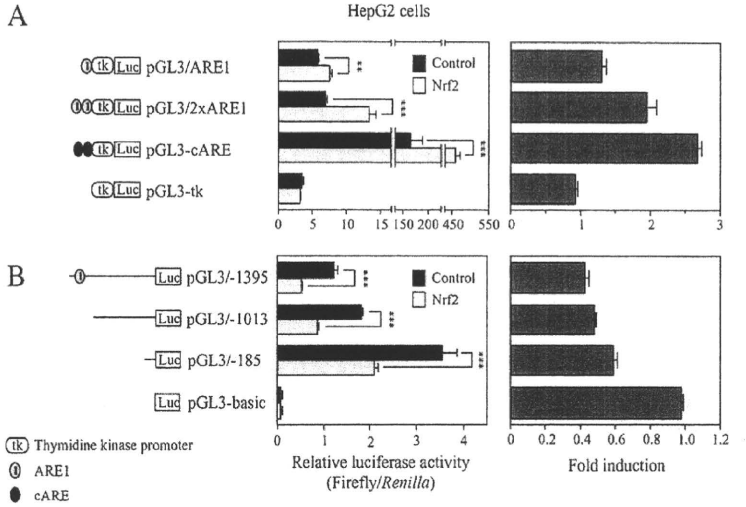

Fig. 4. Effects of overexpression of Nrf2 on CYP2A6 transactivation in HepG2 cells. Reporter plasmids containing ARE sequences (A) or the 5′-flanking region of *CYP2A6* gene with deletion from the 5′ direction (B) were transiently transfected into HepG2 cells with Nrf2 expression plasmid (Nrf2) or pTARGET empty vector (control). The pGL3-cARE plasmid, which contains two copies of the cARE on the human *NQO-1* gene, was used as a positive control. The firefly luciferase activities were normalized with the *Renilla* luciferase activities. Right panel shows the fold induction of the transcriptional activity by the overexpression of Nrf2. Each column represents the mean ± SD of three independent experiments. $^{**}P < 0.01$ and $^{***}P < 0.001$ compared with control.

hepatic transcription factors, which is unlikely the case in cell lines. When the pGL3-cARE plasmid was injected into mice, the luciferase activity in the liver was significantly ($P < 0.05$) increased up to 2.1-fold by SFN treatment (Fig. 5A). It was confirmed that under this condition the endogenous mouse NQO1 mRNA level was significantly ($P < 0.001$) induced (2.4-fold) (Fig. 5B). The luciferase activity of the pGL3/−1395 plasmid containing ARE1 was significantly ($P < 0.05$) increased (1.9-fold) by SFN treatment, but that of the pGL3/−1013 plasmid was not (Fig. 5A). These results suggest that the CYP2A6 promoter containing ARE1 is transactivated by SFN in vivo.

4. Discussion

In the present study, we found that Nrf2 is involved in the regulation of human CYP2A6. Concerning the role of Nrf2 in the regulation of P450, mouse Cyp2a5 was the first reported case [12]. In addition, a recent study demonstrated that human CYP2J2 is regulated by Nrf2 [21]. We could provide evidence to put CYP2A6 into the short list of P450 s that are regulated by Nrf2. It was clearly demonstrated that sulforaphane significantly increased the CYP2A6 mRNA level in human hepatocytes. Sulforaphane, an activator of Nrf2, is contained in cruciferous vegetables such as broccoli sprouts,

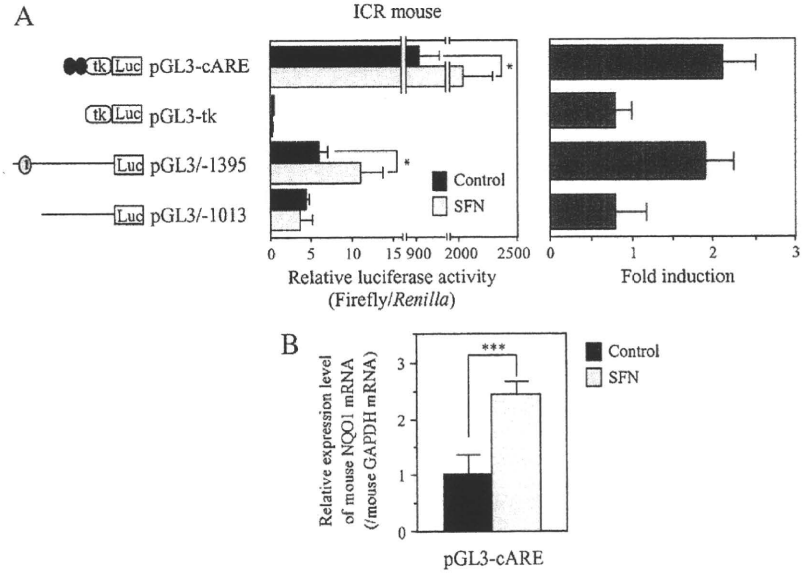

Fig. 5. Effects of SFN on CYP2A6 transactivation in in vivo mice liver transfections. Ten μg of pGL3 reporter plasmid and 1 μg of pGL4.74 plasmid were injected into the tail vein of male ICR mice. After 18 h, 1 mg/head SFN was intraperitoneally administered. After 6 h, the liver was removed and the homogenate and total RNA were prepared for the luciferase assay and real-time RT-PCR, respectively. (A) The firefly luciferase activities were normalized with the *Renilla* luciferase activities. Right panel shows the fold induction of the transcriptional activity by the treatment with SFN. Each column represents the mean ± SD ($n = 3$). $^{*}P < 0.05$ compared with control. (B) NQO1 mRNA levels in mice injected with pGL3-cARE plasmid were determined by real-time RT-PCR. The NQO1 mRNA levels were normalized with the GAPDH mRNA levels. Each column represents the mean ± SD ($n = 3$). $^{***}P < 0.001$ compared with saline.

horseradish, cabbage, and watercress. Interestingly, it has been reported that CYP2A6 activities were significantly increased after the consumption broccoli (500 g/day for 6 days) by 1.4- to 5.5-fold [14]. We believe that the present study may demonstrate the underlying molecular mechanism of the induction.

Electrophoretic mobility shift assays clearly demonstrated that Nrf2 directly bound to ARE1, but not ARE2 and ARE3, on the human *CYP2A6* gene. Previously, Abu-Bakar et al. [22] identified ARE (TGACagaGCA) at −2377 on the 5′-flanking region of the mouse *Cyp2a5* gene to which Nrf2 bound. Interestingly, the sequence of human ARE1 (TGACaaaGCA) has only one base difference with the mouse ARE. Although the core sequence of ARE2 (TGACctgGCc) is similar to that of ARE1, Nrf2 did not bind to ARE2. Thus, the differences in core sequence (underlined) might also be important for the binding of Nrf2. For the supershift assay, we used two kinds of anti-Nrf2 antibody (C-20 and H-300). The supershifted band was observed with the anti-Nrf2 antibody (C-20) but not with the anti-Nrf2 antibody (H-300). Anti-Nrf2 antibody (C-20) recognizes the C-terminal of Nrf2, whereas anti-Nrf2 antibody (H-300) recognizes the N-terminal. Since the N-terminal has a DNA-binding domain, the anti-Nrf2 antibody (H-300) seemed to interfere with the binding of Nrf2 to the DNA, not forming the antibody-Nrf2-DNA complex represented as a supershifted band.

In the luciferase assays, we first determined the effects of the treatment with SFN on the transactivity of the constructs. Unexpectedly, SFN treatment significantly decreased the firefly and *Renilla* luciferase activities derived from the pGL3-tk and phRL-TK plasmids, respectively by approximately half (data not shown). Such a phenomenon was not observed when Nrf2 was over-expressed. It was assumed that SFN might affect the thymidine kinase promoter activities independently of Nrf2. By the over-expression of Nrf2, we found that ARE1 itself was functional for the transactivation. However, the luciferase activities of plasmids containing the intact 5′-flanking region of *CYP2A6* gene were not increased by the overexpression of Nrf2, even if it contained the ARE1. Similar results were obtained using HeLa cells (data not shown), suggesting that it was not a HepG2-specific phenomenon. It was considered that the sequences surrounding ARE may interfere the binding of Nr2, or these cell lines might lack some transcriptional factor(s) that are necessary for the transactivation of CYP2A6. It has been reported that the transactivity of the CYP2C8 promoter was successfully evaluated by the injection of the constructs in mouse in vivo, although such evaluation was unsuccessful in HepG2 cells [23]. Based on this report, we also performed the luciferase assay in mice in vivo and found that the SFN treatment significantly increased the transactivity of the pGL3/−1395 plasmid containing ARE1 (Fig. 5A). Thus, it was concluded that CYP2A6 is regulated by Nrf2 via ARE1.

CYP2A6 is responsible for nicotine metabolism [2]. Smokers adapt their smoking behavior to maintain their nicotine levels in the body [24]. Since the metabolism of nicotine by CYP2A6 is the principal pathway by which nicotine is removed from the circulation, an association between the CYP2A6 activity and cigarette consumption has been suggested [5,6]. Cigarette smoking is known to cause oxidative stress, which activates Nrf2 [25,26]. In addition, tobacco is a substantial source of cadmium, supported by the fact that the serum cadmium level of smokers is 3-folds higher than that of non-smokers [27]. Therefore, it is surmised that the CYP2A6 expression level might be higher in smokers than in non-smokers, although there is no report comparing the expression level of hepatic CYP2A6 protein in smokers versus that in non-smokers. In contrast, it has been reported that in vivo nicotine clearance [28] and in vivo coumarin metabolism [29] were lower in smokers than in non-smokers, suggesting the possibility that some constituents in tobacco smoke might have inhibitory effects on the CYP2A6 activity. Such inhibitory effects could possibly mask the induction of CYP2A6, resulting in decreased in vivo metabolic potency. Thus, it would be of interest to compare the hepatic CYP2A6 expression levels in smokers and non-smokers, although it has been reported that the administration of nicotine itself downregulated CYP2A6-like enzyme expression in African green monkeys [30].

In conclusion, we found that Nrf2 regulates the human CYP2A6. This mechanism implies the possibility that the CYP2A6 expression may be increased by oxidative stress such as by cigarette smoking.

Acknowledgements

This work was supported in part by a grant from the Smoking Research Foundation in Japan. We acknowledge Mr. Brent Bell for reviewing the manuscript.

References

[1] Yun CH, Shimada T, Guengerich FP. Purification and characterization of human liver microsomal cytochrome P-450 2A6. Mol Pharmacol 1991;40:679–85.
[2] Nakajima M, Yamamoto T, Nunoya K, Yokoi T, Nagashima K, Inoue K, et al. Role of human cytochrome P4502A6 in C-oxidation of nicotine. Drug Metab Dispos 1996;24:1212–7.
[3] Nakajima M, Yamamoto T, Nunoya K, Yokoi T, Nagashima K, Inoue K, et al. Characterization of CYP2A6 involved in 3′-hydroxylation of cotinine in human liver microsomes. J Pharmacol Exp Ther 1996;277:1010–5.
[4] Tiano HF, Hosokawa M, Chulada PC, Smith PB, Wang RL, Gonzalez FJ, et al. Retroviral mediated expression of human cytochrome P450 2A6 in C3H/10T1/2 cells confers transformability by 4-(methylnitrosamino)-1-(3-pyridyl)-1-butanone (NNK). Carcinogenesis 1993;14:1421–7.
[5] Nakajima M. Smoking behavior and related cancers: the role of CYP2A6 polymorphisms. Curr Opin Mol Ther 2007;9:538–44.
[6] Strasser AA, Malaiyandi V, Hoffmann E, Tyndale RF, Lerman C. An association of CYP2A6 genotype and smoking topography. Nicotine Tob Res 2007;9:511–8.
[7] Fujieda M, Yamazaki H, Saito T, Kiyotani K, Gyamfi MA, Sakurai M, et al. Evaluation of CYP2A6 genetic polymorphisms as determinants of smoking behavior and tobacco-related lung cancer risk in male Japanese smokers. Carcinogenesis 2004;25:2451–8.
[8] Itoh M, Nakajima M, Higashi E, Yoshida R, Nagata K, Yamazoe Y, et al. Induction of human CYP2A6 is mediated by the pregnane X receptor with peroxisome proliferator-activated receptor-γ coactivator 1α. J Pharmacol Exp Ther 2006;319:693–702.
[9] Higashi E, Fukami T, Itoh M, Kyo S, Inoue M, Yokoi T, et al. Human CYP2A6 is induced by estrogen via estrogen receptor. Drug Metab Dispos 2007;35:1935–41.
[10] Onica T, Nichols K, Larin M, Ng L, Maslen A, Dvorak Z, et al. Dexamethasone-mediated up-regulation of human CYP2A6 involves the glucocorticoid receptor and increased binding of hepatic nuclear factor 4 alpha to the proximal promoter. Mol Pharmacol 2008;73:451–60.
[11] Satarug S, Nishijo M, Ujjin P, Vanavanitkun Y, Baker JR, Moore MR. Effects of chronic exposure to low-level cadmium on renal tubular function and CYP2A6-mediated coumarin metabolism in healthy human subjects. Toxicol Lett 2004;148:187–97.
[12] Abu-Bakar A, Satarug S, Marks GC, Lang MA, Moore MR. Acute cadmium chloride administration induces hepatic and renal CYP2A5 mRNA, protein and activity in the mouse: involvement of transcription factor NRF2. Toxicol Lett 2004;148:199–210.
[13] Itoh K, Chiba T, Takahashi S, Ishii T, Igarashi K, Katoh Y, et al. An Nrf2/small Maf heterodimer mediates the induction of phase II detoxifying enzyme genes through antioxidant response elements. Biochem Biophys Res Commun 1997;236:313–22.
[14] Hakooz N, Hamdan I. Effects of dietary broccoli on human in vivo caffeine metabolism: a pilot study on a group of Jordanian volunteers. Curr Drug Metab 2007;8:9–15.
[15] Nakajima M, Itoh M, Sakai H, Fukami T, Katoh M, Yamazaki H, et al. CYP2A13 expressed in human bladder metabolically activates 4-aminobiphenyl. Int J Cancer 2006;119:2520–6.
[16] Tsuchiya Y, Nakajima M, Kyo S, Kanaya T, Inoue M, Yokoi T. Human CYP1B1 is regulated by estradiol via estrogen receptor. Cancer Res 2004;64:3119–25.
[17] Nakamura A, Nakajima M, Higashi E, Yamanaka H, Yokoi T. Genetic polymorphisms in the 5′-flanking region of human UDP-glucuronosyltransferase 2B7 affect the Nrf2-dependent transcriptional regulation. Pharmacogenet Genomics 2008;18:709–20.
[18] Balogun E, Hoque M, Gong P, Killeen E, Green CJ, Foresti R, et al. Curcumin activates the haem oxygenase-1 gene via regulation of Nrf2 and the antioxidant-responsive element. Biochem J 2003;371:887–95.
[19] Innamorato NG, Rojo AI, García-Yagüe AJ, Yamamoto M, de Ceballos ML, Cuadrado A. The transcription factor Nrf2 is a therapeutic target against brain inflammation. J Immunol 2008;181:680–9.

[20] Kong L, Tanito M, Huang Z, Li F, Zhou X, Zaharia A, et al. Delay of photoreceptor degeneration in tubby mouse by sulforaphane. J Neurochem 2007;101:1041–52.
[21] Lee AC, Murray M. Up-regulation of human CYP2J2 in HepG2 cells by butylated hydroxyanisole is mediated by c-Jun and Nrf2. Mol Pharmacol 2010;77:987–94.
[22] Abu-Bakar A, Lämsä V, Arpiainen S, Moore MR, Lang MA, Hakkola J. Regulation of CYP2A5 gene by the transcription factor nuclear factor (erythroid-derived 2)-like 2. Drug Metab Dispos 2007;35:787–94.
[23] Rodríguez-Antona C, Niemi M, Backman JT, Kajosaari LI, Neuvonen PJ, Robledo M, et al. Characterization of novel CYP2C8 haplotypes and their contribution to paclitaxel and repaglinide metabolism. Pharmacogenomics J 2008;8:268–77.
[24] Benowitz NL. Pharmacology of nicotine: addiction and therapeutics. Annu Rev Pharmacol Toxicol 1996;36:597–613.
[25] Hübner RH, Schwartz JD, De Bishnu P, Ferris B, Omberg L, Mezey JG, et al. Coordinate control of expression of Nrf2-modulated genes in the human small airway epithelium is highly responsive to cigarette smoking. Mol Med 2009;15:203–19.
[26] Boutten A, Goven D, Boczkowski J, Bonay M. Oxidative stress targets in pulmonary emphysema: focus on the Nrf2 pathway. Expert Opin Ther Targets 2010;14:329–46.
[27] Anetor JI, Ajose F, Anetor GO, Iyanda AA, Babalola OO, Adeniyi FA. High cadmium/zinc ratio in cigarette smokers: potential implications as a biomarker of risk of prostate cancer. Niger J Physiol Sci 2008;23:41–9.
[28] Benowitz NL, Jacob III P. Nicotine and cotinine elimination pharmacokinetics in smokers and nonsmokers. Clin Pharmacol Ther 1993;53:316–23.
[29] Poland RE, Pechnick RN, Cloak CC, Wan YJ, Nuccio I, Lin KM. Effect of cigarette smoking on coumarin metabolism in humans. Nicotine Tob Res 2000;2:351–4.
[30] Schoedel KA, Sellers EM, Palmour R, Tyndale RF. Down-regulation of hepatic nicotine metabolism and a CYP2A6-like enzyme in African green monkeys after long-term nicotine administration. Mol Pharmacol 2003;63:96–104.

0090-9556/11/3901-54–60$20.00
DRUG METABOLISM AND DISPOSITION
Copyright © 2011 by The American Society for Pharmacology and Experimental Therapeutics
DMD 39:54–60, 2011

Vol. 39, No. 1
35600/3650890
Printed in U.S.A.

Toxicological Evaluation of Acyl Glucuronides of Nonsteroidal Anti-Inflammatory Drugs Using Human Embryonic Kidney 293 Cells Stably Expressing Human UDP-Glucuronosyltransferase and Human Hepatocytes[S]

Toshihisa Koga, Ryoichi Fujiwara, Miki Nakajima, and Tsuyoshi Yokoi

Drug Metabolism and Toxicology, Faculty of Pharmaceutical Sciences, Kanazawa University, Kanazawa, Japan

Received July 23, 2010; accepted October 6, 2010

ABSTRACT:

The chemical reactivity of acyl glucuronide (AG) has been thought to be associated with the toxic properties of drugs containing carboxylic acid moieties, but there has been no direct evidence that AG formation was related to the toxicity. In the present study, the cytotoxicity and genotoxicity of AGs were investigated. Human embryonic kidney (HEK) 293 cells stably expressing UDP-glucuronosyltransferase (UGT) 1A3 (HEK/UGT1A3) were constructed to assess the cytotoxicity of AGs, and HEK/UGT1A4 cells were also used as a negative reference. After exposure to nonsteroidal anti-inflammatory drugs (NSAIDs) such as naproxen (1 mM), diclofenac (0.1 mM), ketoprofen (1 mM), or ibuprofen (1 mM) for 24 h, HEK/UGT1A3 cells produced AG in a time-dependent manner. However, HEK/UGT1A4 cells hardly produced AG. The cytotoxicity of HEK/UGT1A3 cells was not increased compared with that of HEK/UGT1A4 cells. In addition, the AG formed in NSAID-treated human hepatocytes was decreased from one-third to one-ninth by treatment with (−)-borneol, an inhibitor of acyl glucuronidation, but the cytotoxicity was increased. These results indicated that AG formation reflected the detoxification process in human hepatocytes. Furthermore, the possibility of genotoxicity from the AG formed in NSAID-treated HEK/UGT cells was investigated by the comet assay, and DNA damage was not detected in any HEK/UGT cell lines. In conclusion, the in vitro cytotoxic and genotoxic effects of the AGs of NSAIDs were investigated and AG was not found to be a causal factor in the toxicity.

Introduction

Some of the most commonly prescribed medications and over-the-counter drugs are carboxylate compounds, including many nonsteroidal anti-inflammatory drugs (NSAIDs) and fibrate lipid-lowering drugs. Approximately 25% of drugs withdrawn from the market around the world because of severe toxicity have been carboxylic acids, such as the NSAIDs ibufenac, zomepirac, bromfenac, suprofen, and benoxaprofen. Among drugs containing carboxylic acid, NSAIDs are associated with some degree of hepatotoxicity, immune cytopenias, and hypersensitivity reactions (Bailey and Dickinson, 2003). However, the essential cause of the toxicity is uncertain because of the structural diversity of NSAIDs. For example, diclofenac is associated with hepatotoxicity with a low incidence of 6 to 18 cases/100,000 person-years (Walker, 1997). Both immunological and nonimmunological mechanisms have been proposed to be responsible for the diclofenac hepatotoxicity (Banks et al., 1995; Wade et al., 1997).

Glucuronidation is one of the most important phase II metabolic pathways for endogenous and exogenous substrates in humans. Because glucuronides usually possess less intrinsic biological or chemical activity than their parent aglycones and are rapidly excreted, glucuronidation is considered to be a detoxification reaction (Shipkova et al., 2003). However, acyl glucuronide (AG), which is characterized by its electrophilic reactivity, has been implicated in a wide range of adverse drug effects including drug hypersensitivity reactions and cellular toxicity (Ritter, 2000). It is well known that AG is unstable in physiological conditions and consequently undergoes hydrolysis or intramolecular rearrangement, which occurs by migration of the drug moiety from the 1-*O*-β position to 2-, 3-, and 4-positions on the glucuronic acid ring (Bailey and Dickinson, 2003; Shipkova et al., 2003). As a result, AG potentially binds to cellular macromolecules covalently and has been suspected to mediate idiosyncratic drug toxicities associated with carboxylic drugs (Boelsterli et al., 1995).

This study was supported by the Ministry of Health, Labor, and Welfare of Japan [Health and Labor Sciences Research Grant H20-B10-G001].

Article, publication date, and citation information can be found at http://dmd.aspetjournals.org.

doi:10.1124/dmd.110.035600.

[S] The online version of this article (available at http://dmd.aspetjournals.org) contains supplemental material.

ABBREVIATIONS: NSAID, nonsteroidal anti-inflammatory drug; AG, acyl glucuronide; UGT, UDP-glucuronosyltransferase; HEK, human embryonic kidney; DMSO, dimethyl sulfoxide; UDPGA, UDP-glucuronic acid; 4-MU, 4-methylumbelliferone; GAPDH, glyceraldehyde-3-phosphate dehydrogenase; PAGE, polyacrylamide gel electrophoresis; PBS, phosphate-buffered saline; HPLC, high-performance liquid chromatography; FBS, fetal bovine serum; DMEM, Dulbecco's modified Eagle's medium; LC, liquid chromatography; MS/MS, tandem mass spectrometry; MTT, 3-(4,5-dimethylthiazol-2-yl)-2,5-diphenyltetrazolium; WST-8, 2-(2-methoxy-4-nitrophenyl)-3-(4-nitrophenyl)-5-(2, 4-disulfophenyl)-2*H*-tetrazolium monosodium salt; LDH, lactic dehydrogenase.

Until now, both direct toxic effects and immune-mediated toxicity have been suggested as possible mechanisms of idiosyncratic liver injury. With direct toxicity, covalent protein binding via AG may disrupt the normal physiological function of a "critical" protein or some critical regulatory pathway, leading to cellular necrosis (Pirmohamed et al., 1996). In addition, it has been reported that electrophilic AG can covalently interact with nucleic acids. For example, clofibrate AG and gemfibrozil AG can form DNA adducts, resulting in genotoxicity that can be measured by the single-cell gel electrophoresis (comet) assay (Sallustio et al., 1997). Furthermore, probenecid and clofibric acid induced DNA damage in isolated hepatocytes and UDP-glucuronosyltransferase (UGT)-transfected HEK293 cells via a glucuronidation-dependent pathway (Sallustio et al., 2006; Southwood et al., 2007). The significance of these finding is not yet clear.

Among UGT isoforms, the glucuronidation of carboxylic acid drugs is mediated by UGT1A3, UGT1A9, or UGT2B7 (Sakaguchi et al., 2004). Of interest, despite high sequence identity (amino acid homology of 93%), human UGT1A3 and UGT1A4 differ in terms of substrate selectivity, i.e., UGT1A3 catalyzes the acyl glucuronidation but UGT1A4 hardly does (Kubota et al., 2007). HEK293 cells can express human recombinant UGTs for cytotoxicity studies and effectively glycosylate them (Nakajima et al., 2010; Nishiyama et al., 2010). Therefore, HEK293 cells stably expressing UGT1A3 (HEK/UGT1A3) and UGT1A4 (HEK/UGT1A4) could be useful for toxicity assessment.

Among the drugs containing the carboxylic acid moieties, naproxen, diclofenac, ketoprofen, and ibuprofen were selected. Naproxen, diclofenac, and ibuprofen infrequently show severe drug-induced liver injury, but ketoprofen almost never does (Cuthbert, 1974; Banks et al., 1995; Boelsterli et al., 1995; Walker, 1997; Riley and Smith, 1998). In addition, these NSAIDs are mainly metabolized to the corresponding AG (Foster et al., 1988; Vree et al., 1993; Castillo and Smith, 1995; Kumar et al., 2002). Direct mechanistic evidence linking the toxicity to the formation of drug-protein adducts is lacking. We focused on toxicity due to cell dysfunction by acyl glucuronide formation. In this study, to clarify whether formation of AG occurred in the cells, rather than exposure to hydrophilic AG from outside the cells, which shows toxicity due to cell dysfunction by the adduct formation in vitro, we investigated the cytotoxicity of the NSAIDs exposed to HEK/UGT1A3 or HEK/UGT1A4 and human hepatocytes. Furthermore, we investigated the genotoxicity of the NSAIDs by using the comet assay.

Materials and Methods

Materials. Ketoprofen, ibuprofen, G418, and dimethyl sulfoxide (DMSO) were purchased from Wako Pure Chemicals (Osaka, Japan). Naproxen acyl-β-D-glucuronide, diclofenac acyl-β-D-glucuronide, ketoprofen acyl-β-D-glucuronide, and ibuprofen acyl-β-D-glucuronide were purchased from Toronto Research Chemicals Inc. (North York, ON, Canada). Naproxen, diclofenac sodium salt, UDP-glucuronic acid (UDPGA), alamethicin, 4-methylumbelliferone (4-MU), 4-MU *O*-glucuronide, and (−)-borneol were purchased from Sigma-Aldrich (St. Louis, MO). Rabbit anti-human UGT1A antibodies were obtained from BD Gentest (Woburn, MA). Rabbit anti-human GAPDH antibodies were purchased from Imgenex (San Diego, CA). IRDye 680-labeled goat anti-rabbit secondary antibody and Odyssey Blocking buffer were obtained from LI-COR Biosciences (Lincoln, NE). Primers were commercially synthesized at Hokkaido System Sciences (Sapporo, Japan). Lipofectamine 2000 was purchased from Invitrogen (Carlsbad, CA). All other chemicals and solvents were of the highest grade or the analytical grade commercially available.

Isolation of Human UGT1A3 and Construction of Expression Vectors. Human UGT1A3 (accession number NM_019093) cDNAs were prepared by a reverse transcription-polymerase chain reaction technique using total RNA from human liver. The primer sequences used in this study were as follows: human UGT1A3ex1 sense primer, 5′-TCTTCTGCTGAGATGGCCAC-3′ and human UGT1Aex5 antisense primer, 5′-GCACTCTGGGGCTGATTAAT-3′. After an initial denaturation at 94°C for 5 min, amplification was performed by denaturation at 94°C for 30 s, annealing at 55°C for 30 s, and extension at 72°C for 90 s for 45 cycles, followed by a final extension at 72°C for 5 min. The polymerase chain reaction products were subcloned into pTARGET Mammalian Expression Vector (Promega, Madison, WI), and the DNA sequences of the inserts were determined using a Thermo Sequenase Cy5.5 Dye Terminator Cycle Sequencing Kit (GE Healthcare, Little Chalfont, Buckinghamshire, UK) with a Long-Read Tower DNA sequencer (GE Healthcare).

Stable Expression of UGT1A3 and UGT1A4 Isoforms in HEK293 Cells. An expression vector for UGT1A3 was constructed. HEK293 cells (American Type Culture Collection, Manassas, VA) were grown in Dulbecco's modified Eagle's medium containing 4.5 g/l glucose, 10 mM HEPES, and 10% fetal bovine serum with 5% CO_2 at 37°C. The cells in 12-well plates were transfected with 1.6 μg of the UGT1A3 expression vector using Lipofectamine 2000. Stable transfectants of UGT1A3 were selected in medium containing 800 mg/l G418. HEK293 cells stably expressing UGT1A4 were previously established in our laboratory (Fujiwara et al., 2007a). The cell lines were incubated with 95% O_2/5% CO_2 at 37°C and split 1:4 every 3 days.

SDS-PAGE and Immunoblotting. Samples were boiled for 3 min in Laemmli sample buffer containing 2-mercaptoethanol and separated on 10% SDS-polyacrylamide gel. The separated proteins were electrotransferred onto a polyvinylidene difluoride membrane (Immobilon-P; Millipore Corporation, Billerica, MA). The membrane was washed with phosphate-buffered saline (PBS) two times and blocked with Odyssey Blocking buffer for 1 h. The membranes were incubated with rabbit anti-human UGT1A polyclonal antibody (1:500) and rabbit anti-human GAPDH antibodies (1:1000) diluted with Odyssey Blocking buffer containing 0.1% Tween 20 for 1 h. The membrane was washed with PBS-T (PBS containing 0.1% Tween 20) four times and incubated with IRDye 680-labeled goat anti-rabbit IgG secondary antibody diluted (1:5000) with PBS-T for 1 h. The densities of the bands were determined using an Odyssey Infrared Imaging System (LI-COR Biosciences).

HPLC Analysis of 4-MU *O*-Glucuronide Formation on UGT1A3. 4-MU *O*-glucuronosyltransferase activity was determined as described previously with slight modifications (Fujiwara et al., 2007a). In brief, a typical incubation mixture (100 μl of total volume) contained 50 mM Tris-HCl buffer (pH 7.4), 10 mM $MgCl_2$, 2.5 mM UDPGA, 25 μg/ml alamethicin, 0.4 mg/ml cell homogenate of UGT1A3, and 1 to 1000 μM 4-MU. The reaction was initiated by the addition of UDPGA after a 3-min preincubation at 37°C. After incubation at 37°C for 30 min, the reaction was terminated by the addition of 100 μl of ice-cold methanol. After removal of the protein by centrifugation at 13,000*g* for 5 min, a 50-μl portion of the sample was subjected to HPLC. The analytical column was a CAPCEL PAK C18 UG120 (4.6 × 150 mm, 5 μm; Shiseido, Tokyo, Japan), and the mobile phase was 30% methanol-20 mM potassium phosphate buffer (pH 4.5). The eluent was monitored at 320 nm. The quantification of 4-MU *O*-glucuronide was performed by comparing the HPLC peak height with that of the authentic standard. Kinetic parameters were estimated from the fitted curve using a computer program (KaleidaGraph; Synergy Software, Reading, PA) designed for nonlinear regression analysis. The following equation was applied for Michaelis-Menten kinetics:

$$V = V_{max} \cdot S/(K_m + S)$$

where V is the velocity of the reaction, S is the substrate concentration, K_m is the Michaelis-Menten constant, and V_{max} is the maximum velocity. Data are expressed as means ± S.D. of triplicate determinations.

In Vitro Studies with HEK/UGT Cells. *Cytotoxicity assay.* HEK/UGT cells were seeded into 96-well microtiter plates layered with 2×10^4 cells/well in 0.1 ml of 0.5% (v/v) FBS supplemented DMEM and were immediately incubated with naproxen (1 mM), diclofenac (0.1 mM), ketoprofen (1 mM), or ibuprofen (1 mM) for 6, 12, or 24 h.

Quantification of the AG metabolites. HEK/UGT cells were seeded into 24-well plates layered with 2×10^5 cells/well in 1 ml of 0.5% (v/v) FBS-supplemented DMEM and were immediately incubated with the NSAIDs for 6, 12, or 24 h. The cultured cells were collected into a clean tube after the specified period and then centrifuged at 3000*g* for 5 min to separate the cultured medium and cell fraction. The cell fraction was suspended with 100 μl of PBS. We confirmed the stability of each AG in the autosampler at 4°C

for 24 h (data not shown). The final concentrations of DMSO in the culture medium did not exceed 0.1%.

In Vitro Studies with Human Hepatocytes. *Cytotoxicity assay.* LiverPool cryopreserved human hepatocytes in suspension (Celsis In Vitro Technologies, Brussels, Belgium) were seeded into collagen-coated 96-well microtiter plates layered with 2×10^4 cells/well in 0.1 ml of 0.5% (v/v) FBS-supplemented HCM culture medium (epidermal growth factor- and antibiotic-free) containing 10 nM estradiol and were immediately preincubated with (−)-borneol (1 mM), an inhibitor of acyl glucuronidation. After 30 min, the cells were incubated with the NSAIDs for 6 h.

Quantification of the NSAIDs and their AG metabolites. Human hepatocytes were seeded into collagen-coated 24-well plates layered with 2×10^5 cells/well in 1 ml of 0.5% (v/v) FBS-supplemented HCM culture medium and were immediately preincubated with (−)-borneol (1 mM). After 30 min, the cells were incubated with 0.5% (v/v) FBS-supplemented HCM culture medium containing the NSAIDs for 6 h. We confirmed the stability of each AG at 4°C for 24 h (data not shown). The final concentrations of DMSO in the culture medium did not exceed 0.2%.

LC-MS/MS Analysis and Preparation of AG Samples. The NSAIDs and their AGs were quantified using PE SCIEX API 2000 LC-MS/MS systems (MDS Sciex, Concord, ON, Canada) equipped with an electrospray ionization interface used to generate negative ions $[M - H]^-$. The test drugs were separated on a ZORBAX SB-C18 column (50 × 2.1 mm, 3.5 μm; Agilent Technologies, Santa Clara, CA). The gradient mobile phase consisted of 0.1% formic acid in purified water and 0.1% formic acid in methanol (80:20 to 10:90, v/v). The mobile phase was eluted at 0.2 ml/min using an Agilent 1100 series pump (Agilent Technologies). The NSAIDs and their AGs were monitored by multiple reaction monitoring using transitions of 229 → 169 (naproxen), 405 → 193 (naproxen AG), 294 → 250 (diclofenac), 470 → 193 (diclofenac AG), 253 → 209 (ketoprofen), 429 → 193 (ketoprofen AG), 205 → 161 (ibuprofen), and 381 → 193 (ibuprofen AG). These drugs were calculated by comparing the peak area to that of the authentic standard. The analytical data were processed using Analyst software (version 1.4.1; Applied Biosystems, Foster City, CA) in the API2000 LC-MS/MS systems.

Fifty microliters of methanol-acetic acid (100:1, v/v) was added to a 50-μl portion of the cell fraction or the cultured medium, and then the mixture was centrifuged at 17,400*g* for 10 min. The supernatant was transferred to a glass vial kept at 4°C in an autosampler, and 20 μl of this solution was injected.

Cytotoxicity Assays. An MTT assay was performed with a Cell Counting Kit-8 (Dojindo Laboratories, Kumamoto, Japan) using water-soluble [2-(2-methoxy-4-nitrophenyl)-3-(4-nitrophenyl)-5-(2, 4-disulfophenyl)-2*H*-tetrazolium monosodium salt] (WST-8). WST-8 produces a water-soluble formazan dye upon reduction in the presence of an electron carrier coupling with mitochondrial dehydrogenases. HEK/UGT cells or human hepatocytes (each 2×10^4 cell/well) were seeded in 96-well plates. After 6, 12, and 24 h of incubation for HEK/UGT cells (or after 6 h of incubation for human hepatocytes), CCK-8 reagent was added, and the absorbance of WST-8 formazan at 450 nm was measured according to the manufacturer's instructions. The percent cell viability was calculated by comparing absorbance of cells with that of the control cells.

Cell viabilities of the HEK/UGT cells and human hepatocytes were also evaluated by the intracellular ATP concentration using a CellTiter-Glo Luminescent Cell Viability Assay (Promega). The luminescence of the oxyluciferin generated was measured in the ATP assay by using an 1420 ARVO MX luminometer (excitation 338 nm and emission 458 nm) (PerkinElmer Life and Analytical Sciences–Wallac Oy, Turku, Finland) according to the manufacturer's instructions. The percent cell viability was calculated by comparing cell luminescence with that of the control cells.

Lactate dehydrogenase (LDH) leakage from HEK/UGT cells was evaluated by a Cytotoxicity Detection Kit–LDH (Roche Diagnostics GmbH, Mannheim, Germany). LDH release was measured photometrically at 490 nm (690 nm reference) according to the manufacturer's instructions. The maximum LDH release control was prepared as well as the timing of the addition of lysis solution (1% Triton X-100) to obtain 100% LDH release. The percentage of LDH release was calculated by comparing the absorbance to the maximum LDH release of the control cells.

Comet Assay. The alkaline version of the comet assay is a sensitive genotoxicity test for the detection of DNA strand breaks. The comet assay is based on the principle that DNA fragments formed via DNA damage can be detected after agarose gel electrophoresis and fluorescent staining (Singh et al., 1988). Moreover, the use of different pH conditions during the cell lysis step allows the detection of different types of DNA damage, including single- and double-strand breaks and alkali-labile sites (Kohn, 1991). The comet assay was performed as follows. In brief, HEK/UGT cells were seeded in 24-well plates 24 h before treatment. Cells were treated for 24 h with 0.5% (v/v) FBS-supplemented DMEM containing either vehicle (0.1% DMSO), 1 mM naproxen, 0.1 mM diclofenac, 1 mM ketoprofen or 1 mM ibuprofen. Microscope slides were prepared by immersion in 0.5% (w/v) normal melting agarose. One volume of cell suspension (100 μl, containing approximately 4×10^5 cells) was mixed with 9 volumes of 0.7% (w/v) low-melting point agarose maintained at 37°C in a water bath, after which 100 μl of the diluted suspension was layered on a precoated slide. The slide was immediately covered with a coverslip and incubated at 4°C to solidify the agarose. After the slides were coated with a third layer of 0.7% (w/v) low-melting point agarose at 4°C for 20 min, the embedded cells were immersed for 1 h at 4°C in cold lysis buffer [2.5 M NaCl, 1% (w/v) sodium *N*-lauroylsarcosinate, 100 mM disodium EDTA, and 10 mM Tris base, pH 10] supplemented with 1% (v/v) Triton X-100 and 10% (v/v) DMSO. The slides were placed in a horizontal electrophoresis assembly containing fresh electrophoresis buffer (100 mM NaOH and 10 mM disodium EDTA). To allow DNA unfolding and unwinding, we left the slides in the buffer for 30 min before electrophoresis. After electrophoretic resolution (300 mA for 20 min) using a recirculating horizontal tank (BE-560; Biocraft, Tokyo, Japan), the slides were washed in neutralizing buffer (0.4 M Tris-HCl, pH 7.5) twice for 5 min each and then were stained with ethidium bromide and examined in a fluorescent microscope (BZ-9000; Keyence Corporation, Osaka, Japan). The resulting photographs of fluorescently labeled comets were scored on the basis of the tail extent moment using CometAnalyzer 1.5 (Youworks Corporation, Tokyo, Japan).

The comet moment was typically determined for 150 to 180 cells per treatment on more than three separate experimental days. Data are presented as medians ± interquartile range.

Statistical Analyses. Data are expressed as the mean ± S.D. of three independent determinations. Statistical significance of the cytotoxicity data were determined by a two-tailed Student's *t* test, and comet data were analyzed using a two-tailed nonparametric Mann-Whitney's *U* test (GraphPad Software Inc., San Diego, CA). $P < 0.05$ was considered statistically significant.

Results

UGT1A3 and UGT1A4 in HEK293 Cells: Expression Levels and Enzyme Activities. To establish the stable cell line expressing UGT1A3, five clones were isolated. Immunoblot analysis revealed that the expression levels of UGT varied among the clones and the clones with the highest UGT1A protein levels were selected (data not shown). The HEK293 expression systems of UGT1A3 (HEK/

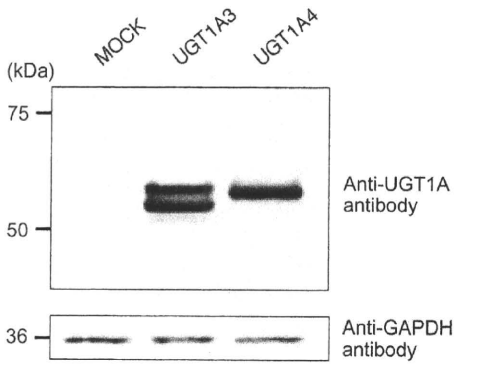

FIG. 1. SDS-PAGE and immunoblot analyses of human UGT1As proteins. Total cell homogenates from HEK/MOCK, HEK/UGT1A3, or HEK/UGT1A4 cells were prepared. The samples (10 μg) were subjected to 10% SDS-PAGE and transferred to a polyvinylidene difluoride membrane. The membrane was probed with an anti-human UGT1A antibody. The UGT1A mRNA levels were corrected with the GAPDH mRNA levels.

TABLE 1

Kinetic parameters for 4-MU O-glucuronidation by UGT1A3 and imipramine N-glucuronidation by UGT1A4 expressed in HEK293 cells

Data represent the mean ± S.D. (n = 3).

UGT Isoform	Glucuronidation	K_m	V_{max}
		mM	*pmol/(min · mg protein)*
UGT1A3	4-MU *O*-glucuronidation	0.3 ± 0.0	640.4 ± 92.1
UGT1A4	Imipramine *N*-glucuronidation	1.1 ± 0.2	240.9 ± 02.9

UGT1A3) or UGT1A4 (HEK/UGT1A4) showed a double band of approximately 54/57 kDa and a single band of approximately 56 kDa, respectively (Fig. 1). As Riedmaier et al. (2010) reported that not only UGT1A3 in human liver microsomes but also recombinant UGT1A3 appeared as a double band of approximately 54/57 kDa, the expression pattern of UGT1A3 was consistent with that of our established UGT1A3. These data indicated that the expressions of UGT1A3 and UGT1A4 were at comparable levels.

After preparation of the total cell homogenate of UGT1A3, the 4-MU *O*-glucuronidation activity was investigated. In our previous study (Fujiwara et al., 2007b), we demonstrated that the total cell homogenate of UGT1A4 could catalyze the *N*-glucuronidation of imipramine. As seen in Table 1, HEK/UGT1A3 and HEK/UGT1A4 showed enzyme activity for each substrate. These data indicated that the enzyme activity of UGT1A3 and UGT1A4 was sufficiently high.

Quantification of AG in HEK/UGT Cells. To investigate the AG formation of each stable cell line, the AG in the cell fraction and the cultured medium was quantified at 6, 12, and 24 h after treatment with the NSAIDs. The AG was not detected in HEK/MOCK and HEK/UGT1A4 cells by LC-MS/MS analysis, whereas it was detected in HEK/UGT1A3 cells (Fig. 2). The AG of naproxen, diclofenac, ketoprofen, and ibuprofen in the cell fraction at 24 h was 4.5 ± 0.8, 3.8 ± 0.4, 0.2 ± 0.1, and 7.2 ± 1.2 pmol/2 × 10^5 cells, respectively, and that in the cultured medium was 137.0 ± 0.8, 104.0 ± 13.1, 6.3 ± 0.7, and 114.7 ± 2.2 pmol/ml, respectively (Supplemental Tables 1-1 and 1-2). Compared with the AG in the cell fraction of HEK/UGT1A3, the AG in the cultured medium was increased in a time-dependent manner. The AG formed in NSAID-treated cells was not accumulated and effectively distributed in the medium.

Cytotoxicity of NSAIDs in HEK/UGT Cells. To investigate the cytotoxicity of the AGs of the NSAIDs, MTT, ATP, and LDH release assays were performed using HEK/UGT cells. In the MTT and ATP assays (Fig. 3), cell viability was decreased time dependently after treatment with the NSAIDs. However, there was no difference in the cell viability of HEK/UGT1A3 cells, which produced the AG, compared with that of HEK/MOCK and/or HEK/UGT1A4 cells. LDH leakage into the cultured medium was also assessed for 6-, 12-, and 24-h incubations. In each HEK/UGT cell line, none of the NSAIDs demonstrated LDH leakage that exceeded 5.4% of the total cell LDH levels (Supplemental Fig. 1). These results indicated that no cytotoxicity due to the AG formation from the NSAIDs was detected in HEK/UGT cells.

In addition, to investigate whether the other substrates affected the cytotoxicity, we used an MTT assay of HEK/UGT cells exposed to other carboxylic acid drugs such as clofibric acid (1 mM), gemfibrozil (1 mM), salicylic acid (1 mM), and zomepirac (0.1 mM) at 24 h. The cell viability of HEK/UGT1A3 cells was not significantly decreased compared with that of HEK/UGT1A4 cells (Supplemental Fig. 2).

Quantification of AG in Human Hepatocytes. To investigate the inhibition effect of (−)-borneol on the formation of AG in NSAID-treated human hepatocytes, the AG in the cell fraction and the cultured medium was quantified. Without (−)-borneol treatment, the AG of naproxen, diclofenac, ketoprofen, and ibuprofen formed in the cell fraction at 6 h was 33.6 ± 1.0, 59.6 ± 1.1, 6.8 ± 0.5, and 27.7 ± 1.6 pmol/2 × 10^5 cells, respectively, and that formed in the cultured medium was 1323.9 ± 44.3, 2816.1 ± 63.5, 436.8 ± 8.0, and 1156.7 ± 21.9 pmol/ml, respectively (Fig. 4). On the other hand, with (−)-borneol treatment, the AG of naproxen, diclofenac, ketoprofen, and ibuprofen formed in the cell fraction at 6 h was 10.3 ± 0.4, 15.1 ± 1.3, 1.7 ± 0.1, and 3.5 ± 0.3 pmol/2 × 10^5 cells, respectively, and that formed in the cultured medium was 393.7 ± 13.7, 610.5 ± 29.7, 54.9 ± 0.8, and 126.5 ± 10.6 pmol/ml, respectively (Fig. 4). Therefore, the AG formed in NSAID-treated human hepatocytes was decreased to one-third to one-ninth by (−)-borneol treatment.

Cytotoxicity of NSAIDs in Human Hepatocytes. We confirmed the inhibition effect of (−)-borneol on the AG formation of the NSAIDs in human hepatocytes. To investigate the effect of AG on the cytotoxicity in human hepatocytes, ATP and MTT assays were performed. In the ATP assay (Fig. 5A), the cell viability without (−)-borneol treatment was significantly decreased in the presence of the NSAIDs except ketoprofen compared with the nontreated control. If the AG showed cytotoxicity, the cell viability would be restored by (−)-borneol treatment. The cell viability with (−)-borneol treatment was further decreased, even though the AG formed in human hepatocytes was decreased. Likewise, MTT assay revealed that the cell viability was significantly decreased in the presence of naproxen (Fig. 5B). (−)-Borneol decreased the cell viability in the presence of diclofenac or ibuprofen. If the AG showed cytotoxicity, the cell viability would be restored by (−)-borneol treatment. However, (−)-borneol unexpectedly decreased the cell viability. To investigate whether the cytotoxicity is due to increased contents of the parent drugs in the cell fraction, we quantified the parent drugs using LC-MS/MS analysis. As a result, the contents of the parent drugs with (−)-borneol treatment were significantly higher than those without (−)-borneol treatment (Fig. 5C). These results indicated that the decreased cell viability of human hepatocytes with (−)-borneol treatment might be due to the increased contents of the parent drugs in the cell fraction. Therefore, AG formed in NSAID-treated human hepatocytes showed no cytotoxicity.

Comet Assay. To investigate the possibility that the AG formed in NSAID-treated HEK/UGT cells caused secondary genotoxicity by nicking DNA, the comet assay was conducted after the 24-h treatment. The scores of the tail moments of NSAID-treated HEK/UGT

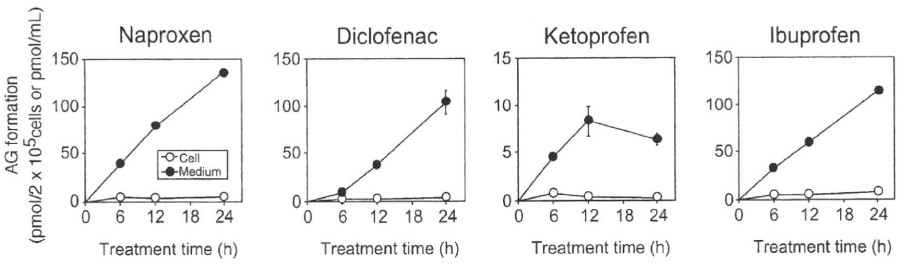

FIG. 2. Time-dependent changes of AG formation in NSAID-treated HEK/UGT1A3 cells. HEK/UGT1A3 cells (2 × 10^5 cells/ml/well) were incubated with naproxen (1 mM), diclofenac (0.1 mM), ketoprofen (1 mM), or ibuprofen (1 mM) for 6, 12, and 24 h. The cell fraction (picomoles per 2 × 10^5 cells) and the cultured medium (picomoles per milliliter) were measured by LC-MS/MS. ○, cell fraction; ●, cultured medium. Each point represents the mean ± S.D. of triplicate determinations.

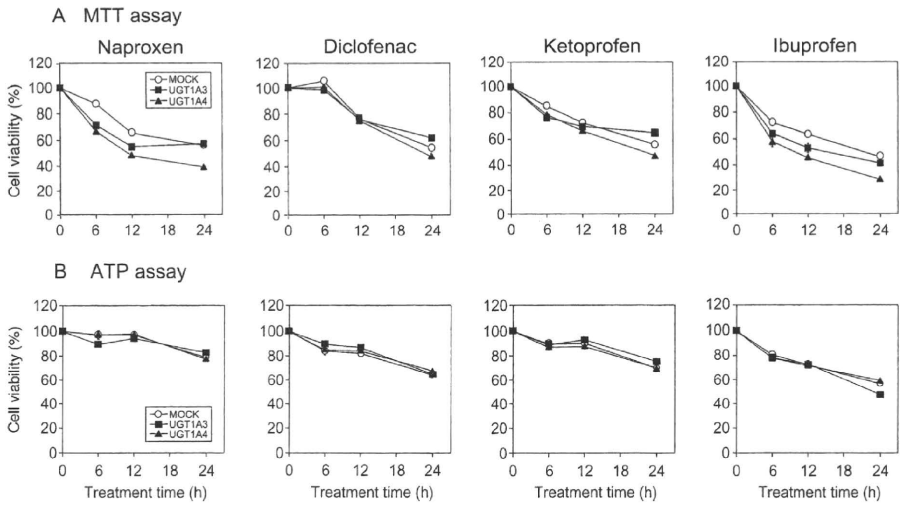

FIG. 3. Time-dependent changes of cell viability assessed by MTT and ATP assays in NSAID-treated HEK/UGT cells. A, MTT assay. B, ATP assay. HEK/UGT cells (2×10^4 cells/0.1 ml/well) were incubated with naproxen (1 mM), diclofenac (0.1 mM), ketoprofen (1 mM), and ibuprofen (1 mM) for 6, 12, and 24 h. ○, MOCK; ■, UGT1A3; ▲, UGT1A4. Each point represents the mean ± S.D. of triplicate determinations.

cells are shown in Fig. 6. Cells exposed to the NSAIDs showed hardly any DNA strand breaks compared with the controls. Methylmethane sulfonate at 0.1 mM, as a positive control, caused a significant increase in DNA migration ($P < 0.001$) compared with the solvent control (DMSO). As shown in Fig. 6B, no drugs significantly increased the DNA migration in HEK/UGT1A3 cells, even though AG was produced in the cells. No genotoxicity owing to the AG formation from the NSAIDs could be detected in the present study.

Discussion

There is increasing evidence that the formation of drug-protein adducts is involved in idiosyncratic reactions. However, direct mechanism-based evidence linking the toxicity to the formation of drug-protein adducts is lacking. We focused in this study on the toxicity due to cell dysfunction by acyl glucuronide formation. Therefore, we investigated whether the acyl glucuronide of NSAIDs represents cytotoxicity directly. In the toxicological assessment of AG in vitro, exposure of the cells to the hydrophilicity of AG must be taken into account, because it is possible that exposure to the AG from outside the cells could result in poor absorption. Therefore, to clarify the toxicity of AG, the cytotoxicity and genotoxicity of the AG formed in NSAID-treated HEK/UGT cells and human hepatocytes were evaluated at high concentrations, but there was no severe cytotoxicity from the parent drugs per se. For example, diclofenac caused low cell viability (approximately 20% of MOCK cells) at 1 mM (data not shown). Therefore, we examined diclofenac toxicity at 0.1 mM. On the other hand, naproxen, ibuprofen, and ketoprofen were examined at 1 mM.

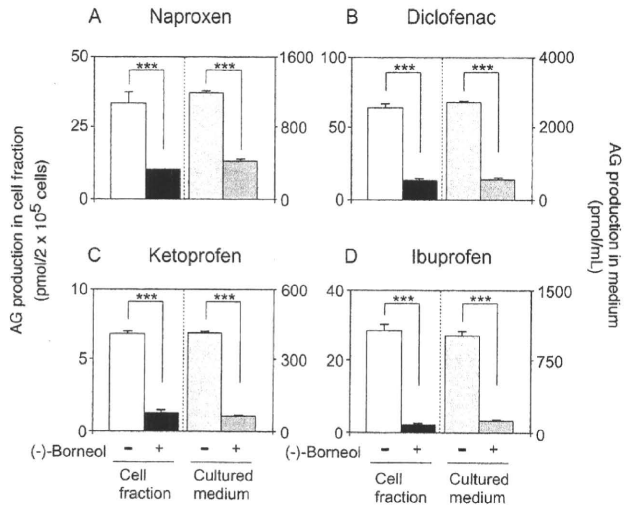

FIG. 4. Effect of (−)-borneol treatment on AG formation in NSAID-treated human hepatocytes. Human hepatocytes (2×10^5 cells/ml/well) treated with 1 mM (−)-borneol for 30 min were incubated with naproxen (1 mM) (A), diclofenac (0.1 mM) (B), ketoprofen (1 mM) (C), or ibuprofen (1 mM) (D) for 6 h. The cell fraction and the cultured medium were measured by LC-MS/MS analysis. Each point represents the mean ± S.D. of triplicate determinations. ***, $P < 0.001$ compared with without (−)-borneol treatment (control).

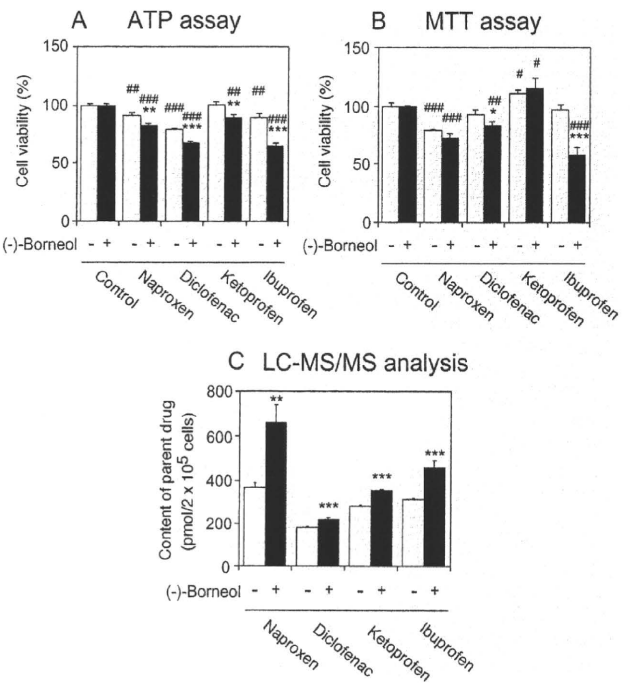

FIG. 5. Effect of (−)-borneol treatment on cell viability assessed by ATP (A) or MTT (B) assays and on contents of parent NSAIDs in the cell fraction (C) of human hepatocytes. The human hepatocytes (2×10^4 cells/0.1 ml/well) treated with 1 mM (−)-borneol for 30 min were incubated with naproxen (1 mM), diclofenac (0.1 mM), ketoprofen (1 mM), or ibuprofen (1 mM) for 6 h. □, without (−)-borneol treatment; ■, with (−)-borneol treatment. Each column represents the mean ± S.D. of triplicate determinations. *, $P < 0.05$; **, $P < 0.01$; ***, $P < 0.001$, compared with without (−)-borneol treatment. #, $P < 0.05$; ##, $P < 0.01$; ###, $P < 0.001$, compared with without NSAID treatment.

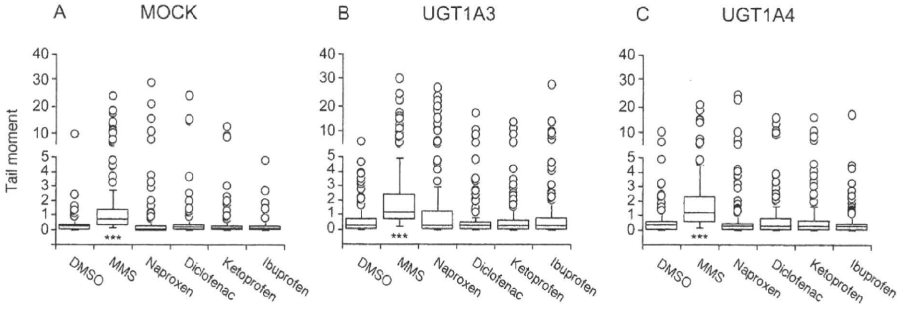

FIG. 6. DNA damage measured by the comet assay in HEK/MOCK (A), HEK/UGT1A3 (B), or HEK/UGT1A4 (C) cells. HEK/UGT cells (2×10^5 cells/ml/well) were incubated with naproxen (1 mM), diclofenac (0.1 mM), ketoprofen (1 mM), ibuprofen (1 mM), and methylmethane sulfonate (MMS) (0.1 mM, as a positive control) for 24 h. Results are shown as median (± interquartile range) tail moment calculated from 30 to 60 comets scored per slide, in more than three separate experiments (total 150–180 comets). ○, outliers. ***, $P < 0.001$ compared with control (DMSO vehicle) incubations.

HEK/UGT1A3 cells were constructed to investigate the cytotoxicity of AG. HEK/UGT1A4 cells were also used as a reference for HEK/UGT1A3 cells. HEK/UGT1A4 cells have the characteristics of high amino acid homology and different catalytic properties compared with HEK/UGT1A3 cells. Moreover, HEK/UGT1A4 cells could reflect the cytotoxicity of AG more accurately than HEK/MOCK cells (Fig. 1). After exposure to the NSAIDs for 24 h, AG formation was only detected in HEK/UGT1A3 cells in a time-dependent manner (Fig. 2). However, there was no difference in the cytotoxicity to HEK/UGT1A3 cells compared with that to HEK/UGT1A4 cells, even though HEK/UGT1A3 cells could produce AG (Fig. 3; Supplemental Fig. 1). Although the cytotoxicity of other carboxylic acid drugs (i.e., clofibric acid, gemfibrozil, salicylic acid, or zomepirac) in HEK/UGT cells was investigated, the cell viability of HEK/UGT1A3 cells was not significantly decreased compared with that of HEK/UGT1A4 cells (Supplemental Fig. 2). Furthermore, the cytotoxicity of other carboxylic acid drugs such as acetylsalicylic acid, flurbiprofen, indomethacin, niflumic acid, mefenamic acid, sulindac, bezafibrate, furosemide, probenecid, or mycophenolic acid at 1 mM was investigated by using the MTT assay, and the cell viability of HEK/UGT1A3 cells was not significantly decreased (data not shown). Therefore, no cytotoxicity of AG was detected even when other carboxylic acid drugs were selected. In general, it has been thought that protein and/or DNA adduct formation in response to AG is a causal factor for toxicity. Therefore, we may not be able to exclude the possibility of increased cytotoxicity after long-term exposure to carboxylic acid drugs. To address this issue, the cytotoxicity was investigated by using the MTT assay after exposure to the drugs (naproxen, ketoprofen, ibuprofen, clofibric acid, gemfibrozil, and salicylic acid at 1 mM and diclofenac and zomepirac at 0.1 mM) for up to 72 h. However, there was no significant difference in the cell viability of the HEK/UGT cells (data not shown).

HEK293 cells have been noted to lack many uptake and efflux transporters that are normally expressed on human hepatocytes. For example, HEK293 cells do not express organic anion-transporting polypeptide 2 or 8 (Hirano et al., 2004), so that the uptake of carboxylic acid drugs may be lower than that in human hepatocytes. Likewise, HEK293 cells do not express multidrug resistance-associated protein 2 (Hagmann et al., 1999) or multidrug resistance-associated protein3 (Zeng et al., 2000), so that the efflux of intracellularly generated AG may be lower than that in human hepatocytes. Therefore, the cytotoxicity of AG was investigated by using human hepatocytes that might reflect more closely AG formation in vivo. The AG formation in human hepatocytes was much higher than that in HEK/UGT1A3 cells. In particular, the AG in the cell fraction of human hepatocytes at 6 h of treatment was approximately 6- to 30-fold that in the cell fraction of HEK/UGT1A3 cells (Figs. 2 and 4). These results suggested that other UGT isoforms (i.e., UGT1A9 and UGT2B7) catalyzing the glucuronidation of the carboxylic acid drugs and/or the transporters involved in the AG formation might be expressed in human hepatocytes. Although the AG formed in NSAID-treated human hepatocytes was decreased by (−)-borneol treatment, the cytotoxicity was increased. The LC-MS/MS analysis indicated that the content of the parent drugs in the cell fraction of human hepatocytes with (−)-borneol treatment was significantly higher than that without (−)-borneol treatment (Fig. 5C). These results suggested that the formation of AG in human hepatocytes might represent a detoxification process.

The comet assay is a unique assay method for assessing the genotoxicity of AG (Sallustio et al., 1997, 2006; Southwood et al., 2007). Thus, we investigated genotoxicity using the comet assay. The results showed that the tail moments of the DNA migration were not significantly different in the HEK/UGT cell lines, even though HEK/UGT1A3 cells produced AG in the presence of the NSAIDs. Therefore, the AG formation from the NSAIDs is not involved in genotoxicity in vitro. In a recent report, Brambilla and Martelli (2009) described the genotoxicity and carcinogenicity of many NSAIDs. According to their report, naproxen, diclofenac, ketoprofen, and ibuprofen gave negative responses in reverse mutation (Ames) tests with *Salmonella typhimurium* and in a long-term carcinogenesis assay using rats and mice. Our results showing a lack of genotoxicity for all four NSAIDs by the comet assay are in accordance with this report. On the other hand, clofibric acid (1 mM), which produced no AG metabolites, gave significantly positive results for genotoxicity by the comet assay using HEK/UGT1A3 cells at 24 h of treatment (data not shown). This result supported the previous report of Southwood et al. (2007). As described in this report, fibrate hypolipidemic agents such as clofibric acid are nongenotoxic (Ashby et al., 1994). Therefore, one should be careful in interpreting the results of the comet assay.

Among the NSAIDS containing carboxylic acid drugs, diclofenac AG is one of the most studied for its related toxicity. Diclofenac AG is excreted into bile and transported to the small intestine where it can produce erosions and ulcers in a dose-dependent manner (Seitz and Boelsterli, 1998). In a recent article, Lagas et al. (2010) reported that *Mrp2/Mrp3/Bcrp1*$^{-/-}$ mice have markedly elevated levels of diclofenac AG in their liver and display acute, albeit mild, hepatotoxicity. As for the metabolic activation, it is well known that diclofenac is converted to 4′-hydroxydiclofenac and 5-hydroxydiclofenac via direct hydroxylation and that these two metabolites are further oxidized to form benzoquinone imine intermediates by human CYP2C9 and CYP3A4, respectively (Tang et al., 1999). Quinone imines are electrophiles that have been generally implicated in redox cycling and in producing oxidative stress and can undergo covalent binding with nonprotein or protein sulfhydryl groups because of their thiol reactivity (Boelsterli, 2003). Given the toxicity of diclofenac, it seemed to be important to evaluate not only the AG but also the quinone imines of diclofenac.

In conclusion, we investigated the relationship between cytotoxicity and AG formation by NSAIDs (naproxen, diclofenac, ketoprofen, and ibuprofen) in HEK/UGT cells and human hepatocytes and also the genotoxicity of the AG from NSAIDs in HEK/UGT cells. However,

no cytotoxicity or genotoxicity due to the AG formed in the cells was found in the present study. Therefore, because AG appeared not to be a causal factor of the toxicity in vitro, additional work addressing a possible immune-mediated toxicity will be needed to clarify the toxicity of AG. This study provides new insight into the evaluation of acyl glucuronide toxicity in drug development.

Acknowledgments

We acknowledge Dr. Tetsushi Watanabe (Kyoto Pharmaceutical University) for technical teaching and discussion about the comet assay and Brent Bell for reviewing the manuscript.

Authorship Contributions

Participated in research design: Koga, Nakajima, and Yokoi.
Conducted experiments: Koga.
Contributed new reagents or analytic tools: Koga and Fujiwara.
Performed data analysis: Koga.
Wrote or contributed to the writing of the manuscript: Koga and Yokoi.

References

Ashby J, Brady A, Elcombe CR, Elliot BM, Ishamael J, Odum J, Tugwood JD, Kettle S, and Purchase IFH (1994) Mechanistically-based human hazard assessment of peroxisome proliferator-induced hepatocarcinogenesis. *Hum Exp Toxicol* **13 (Suppl 2):**S1–S117.

Bailey MJ and Dickinson RG (2003) Acyl glucuronide reactivity in perspective: biological consequences. *Chem Biol Interact* **145:**117–137.

Banks AT, Zimmerman HJ, Ishak KG, and Harter JG (1995) Diclofenac-associated hepatotoxicity: analysis of 180 cases reported to the Food and Drug Administration as adverse reactions. *Hepatology* **22:**820–827.

Boelsterli UA (2003) Diclofenac-induced liver injury: a paradigm of idiosyncratic drug toxicity. *Toxicol Appl Pharmacol* **192:**307–322.

Boelsterli UA, Zimmerman HJ, and Kretz-Rommel A (1995) Idiosyncratic liver toxicity of nonsteroidal antiinflammatory drugs: molecular mechanisms and pathology. *Crit Rev Toxicol* **25:**207–235.

Brambilla G and Martelli A (2009) Genotoxicity and carcinogenicity studies of analgesics, anti-inflammatory drugs and antipyretics. *Pharmacol Res* **60:**1–17.

Castillo M and Smith PC (1995) Disposition and reactivity of ibuprofen and ibufenac acyl glucuronides in vivo in the rhesus monkey and in vitro with human serum albumin. *Drug Metab Dispos* **23:**566–572.

Cuthbert MF (1974) Adverse reactions to non-steroidal antirheumatic drugs. *Curr Med Res Opin* **2:**600–610.

Foster RT, Jamali F, Russell AS, and Alballa SR (1988) Pharmacokinetics of ketoprofen enantiomers in young and elderly arthritic patients following single and multiple doses. *J Pharm Sci* **77:**191–195.

Fujiwara R, Nakajima M, Yamanaka H, Nakamura A, Katoh M, Ikushiro S, Sakaki T, and Yokoi T (2007a) Effects of coexpression of UGT1A9 on enzymatic activities of human UGT1A isoforms. *Drug Metab Dispos* **35:**747–757.

Fujiwara R, Nakajima M, Yamanaka H, Katoh M, and Yokoi T (2007b) Interactions between human UGT1A1, UGT1A4, and UGT1A6 affect their enzymatic activities. *Drug Metab Dispos* **35:**1781–1787.

Hagmann W, Nies AT, König J, Frey M, Zentgraf H, and Keppler D (1999) Purification of the human apical conjugate export pump MRP2 reconstitution and functional characterization as substrate-stimulated ATPase. *Eur J Biochem* **265:**281–289.

Hirano M, Maeda K, Shitara Y, and Sugiyama Y (2004) Contribution of OATP2 (OATP1B1) and OATP8 (OATP1B3) to the hepatic uptake of pitavastatin in humans. *J Pharmacol Exp Ther* **311:**139–146.

Kohn KW (1991) Principles and practice of DNA filter elution. *Pharmacol Ther* **49:**55–77.

Kubota T, Lewis BC, Elliot DJ, Mackenzie PI, and Miners JO (2007) Critical roles of residues 36 and 40 in the phenol and tertiary amine aglycone substrate selectivities of UDP-glucuronosyltransferases 1A3 and 1A4. *Mol Pharmacol* **72:**1054–1062.

Kumar S, Samuel K, Subramanian R, Braun MP, Stearns RA, Chiu SH, Evans DC, and Baillie TA (2002) Extrapolation of diclofenac clearance from in vitro microsomal metabolism data: role of acyl glucuronidation and sequential oxidative metabolism of the acyl glucuronide. *J Pharmacol Exp Ther* **303:**969–978.

Lagas JS, Sparidans RW, Wagenaar E, Beijnen JH, and Schinkel AH (2010) Hepatic clearance of reactive glucuronide metabolites of diclofenac in the mouse is dependent on multiple ATP-binding cassette efflux transporters. *Mol Pharmacol* **77:**687–694.

Nakajima M, Koga T, Sakai H, Yamanaka H, Fujiwara R, and Yokoi T (2010) *N*-Glycosylation plays a role in protein folding of human UGT1A9. *Biochem Pharmacol* **79:**1165–1172.

Nishiyama T, Izawa T, Usami M, Ohnuma T, Ogura K, and Hiratsuka A (2010) Cooperation of NAD(P)H:quinone oxidoreductase 1 and UDP-glucuronosyltransferases reduces menadione cytotoxicity in HEK293 cells. *Biochem Biophys Res Commun* **394:**459–463.

Pirmohamed M, Madden S, and Park BK (1996) Idiosyncratic drug reactions. Metabolic bioactivation as a pathogenic mechanism. *Clin Pharmacokinet* **31:**215–230.

Riedmaier S, Klein K, Hofmann U, Keskitalo JE, Neuvonen PJ, Schwab M, Niemi M, and Zanger UM (2010) UDP-glucuronosyltransferase (UGT) polymorphisms affect atorvastatin lactonization in vitro and in vivo. *Clin Pharmacol Ther* **87:**65–73.

Riley TR 3rd and Smith JP (1998) Ibuprofen-induced hepatotoxicity in patients with chronic hepatitis C: a case series. *Am J Gastroenterol* **93:**1563–1565.

Ritter JK (2000) Roles of glucuronidation and UDP-glucuronosyltransferases in xenobiotic bioactivation reactions. *Chem Biol Interact* **129:**171–193.

Sakaguchi K, Green M, Stock N, Reger TS, Zunic J, and King C (2004) Glucuronidation of carboxylic acid containing compounds by UDP-glucuronosyltransferase isoforms. *Arch Biochem Biophys* **424:**219–225.

Sallustio BC, Degraaf YC, Weekley JS, and Burcham PC (2006) Bioactivation of carboxylic acid compounds by UDP-glucuronosyltransferases to DNA-damaging intermediates: role of glycoxidation and oxidative stress in genotoxicity. *Chem Res Toxicol* **19:**683–691.

Sallustio BC, Harkin LA, Mann MC, Krivickas SJ, and Burcham PC (1997) Genotoxicity of acyl glucuronide metabolites formed from clofibric acid and gemfibrozil: a novel role for phase-II-mediated bioactivation in the hepatocarcinogenicity of the parent aglycones? *Toxicol Appl Pharmacol* **147:**459–464.

Seitz S and Boelsterli UA (1998) Diclofenac acyl glucuronide, a major biliary metabolite, is directly involved in small intestinal injury in rats. *Gastroenterology* **115:**1476–1482.

Shipkova M, Armstrong VW, Oellerich M, and Wieland E (2003) Acyl glucuronide drug metabolites: toxicological and analytical implications. *Ther Drug Monit* **25:**1–16.

Singh NP, McCoy MT, Tice RR, and Schneider EL (1988) A simple technique for quantitation of low levels of DNA damage in individual cells. *Exp Cell Res* **175:**184–191.

Southwood HT, DeGraaf YC, Mackenzie PI, Miners JO, Burcham PC, and Sallustio BC (2007) Carboxylic acid drug-induced DNA nicking in HEK293 cells expressing human UDP-glucuronosyltransferases: role of acyl glucuronide metabolites and glycation pathways. *Chem Res Toxicol* **20:**1520–1527.

Tang W, Stearns RA, Wang RW, Chiu SH, and Baillie TA (1999) Roles of human hepatic cytochrome P450s 2C9 and 3A4 in the metabolic activation of diclofenac. *Chem Res Toxicol* **12:**192–199.

Vree TB, Van Den Biggelaar-Martea M, Verwey-Van Wissen CP, Vree ML, and Guelen PJ (1993) The pharmacokinetics of naproxen, its metabolite *O*-desmethylnaproxen, and their acyl glucuronides in humans. Effect of cimetidine. *Br J Clin Pharmacol* **35:**467–472.

Wade LT, Kenna JG, and Caldwell J (1997) Immunochemical identification of mouse hepatic protein adducts derived from the nonsteroidal anti-inflammatory drugs diclofenac, sulindac, and ibuprofen. *Chem Res Toxicol* **10:**546–555.

Walker AM (1997) Quantitative studies of the risk of serious hepatic injury in persons using nonsteroidal antiinflammatory drugs. *Arthritis Rheum* **40:**201–208.

Zeng H, Liu G, Rea PA, and Kruh GD (2000) Transport of amphipathic anions by human multidrug resistance protein 3. *Cancer Res* **60:**4779–4784.

Address correspondence to: Dr. Yokoi Tsuyoshi, Drug Metabolism and Toxicology, Faculty of Pharmaceutical Sciences, Kanazawa University, Kakuma-machi, Kanazawa 920-1192, Japan. E-mail: tyokoi@kenroku.kanazawa-u.ac.jp

Toxicology Letters 200 (2011) 139–145

Contents lists available at ScienceDirect

Toxicology Letters

journal homepage: www.elsevier.com/locate/toxlet

IL-4 mediates dicloxacillin-induced liver injury in mice

Satonori Higuchi[a], Masanori Kobayashi[a], Yukitaka Yoshikawa[a], Koichi Tsuneyama[b], Tatsuki Fukami[a], Miki Nakajima[a], Tsuyoshi Yokoi[a,*]

[a] Drug Metabolism and Toxicology, Faculty of Pharmaceutical Sciences, Kanazawa University, Kakuma-machi, Kanazawa 920-1192, Japan
[b] Department of Diagnostic Pathology, Graduate School of Medicine and Pharmaceutical Science for Research, University of Toyama, Sugitani, 930-0194 Toyama, Japan

ARTICLE INFO

Article history:
Received 18 September 2010
Received in revised form
10 November 2010
Accepted 11 November 2010
Available online 19 November 2010

Keywords:
13,14-Dihydro-15-keto-prostaglandin D_2
Drug-induced liver injury
IL-4

ABSTRACT

Drug-induced liver injury (DILI) is a major problem in drug development and clinical drug therapy. In most cases, the mechanisms are still unknown. It is difficult to predict DILI in humans due to the lack of experimental animal models. Dicloxacillin, penicillinase-sensitive penicillin, rarely causes cholestatic or mixed liver injury, and there is some evidence for immunoallergic idiosyncratic reaction in human. In this study, we investigated the mechanisms of dicloxacillin-induced liver injury. Plasma ALT and total-bilirubin (T-Bil) levels were significantly increased in dicloxacillin-administered (600 mg/kg, i.p.) mice. Dicloxacillin administration induced Th2 (helper T cells)-mediated factors and increased the plasma interleukin (IL)-4 level. Neutralization of IL-4 suppressed the hepatotoxicity of dicloxacillin, and recombinant mouse IL-4 administration (0.5 or 2.0 μg/mouse, i.p.) exacerbated it. Chemoattractant receptor-homologous molecule expressed on Th2 cells (CRTh2) is a cognate receptor for prostaglandin (PG) D_2, and is suggested to be involved in Th2-dependent allergic inflammation. We investigated the effect of 13,14-Dihydro-15-keto-PGD_2 (DK-PGD_2; 10 μg/mouse, i.p.) administration on dicloxacillin-induced liver injury. DK-PGD_2/dicloxacillin coadministration resulted in a significant increase of alanine aminotransferases and a remarkable increase of macrophage inflammatory protein 2 expression. In conclusion, to the best of our knowledge, this is the first report to demonstrate that dicloxacillin-induced liver injury is mediated by a Th2-type immune reaction and exacerbated by DK-PGD_2.

© 2010 Elsevier Ireland Ltd. All rights reserved.

1. Introduction

Drug-induced liver injury (DILI) is the most frequent reason for the withdrawal of an approved drug from the market and for failures in drug development in pharmaceutical companies. Because of DILI, several drugs have been removed from the pharmaceutical market, including bromfenac, ebrotidine, and troglitazone (Holt and Ju, 2006). In most cases, the mechanisms of DILI are unknown and predictive experimental animal models are lacking.

Adverse effects of antibiotics are variable and can induce phlebitis, hypersensitivity reactions, changes in microbial flora, adverse interactions with other drugs as well as liver injury (Stein, 2005). It has been reported that there are many case reports of DILI due to antibiotics administration (Bjornsson and Olsson, 2005), however there are a few reports of pathological investigations. Dicloxacillin and penicillinase-sensitive penicillin rarely cause liver injury and there is some evidence for an immunoallergic idiosyncratic reaction. Dicloxacillin induced cholestasis with a moderate inflammatory reaction, allergic symptoms and infiltration of mononuclear cells, such as neutrophils and eosinophils, were demonstrated in many cases (Olsson et al., 1992). Allergic symptoms and eosinophilia are generally induced by Th2 cytokines (Kay, 2001). From these lines of evidences, we hypothesized that Th2 factors might involve in dicloxacillin-induced liver injury.

T cell-mediated immune responses play pivotal roles in the pathogenesis of a variety of human liver disorders (Kita et al., 2001; Heneghan and McFarlane, 2002; Holt and Ju, 2006). The action of T cells in the liver is mediated through the release of a variety of cytokines, which target liver cells and immune cells by activating multiple signaling cascades, including the signal transducers and activators of transcription factor (STAT) family members (Leonard and O'Shea, 1998). STAT6 is specifically activated by interleukin (IL)-4, which plays important roles in Th2 differentiation, tissue adhesion, and inflammation (Jaruga et al., 2003; Nelms et al., 1999). Th cells are subdivided into Th1, Th2, and Th17 subsets by their unique production of cytokines and characteristic transcription factors. Th1 cells require "T-box expressed in T cells" (T-bet) and secrete interferon (IFN)-γ. In contrast, Th2 cells require GATA-binding domain-3 (GATA-3) and produce IL-4, IL-5 and IL-13. Retinoid-related orphan receptor γt (ROR-γt) is indispensable for the differentiation of Th17 cells which mainly secret IL-17 and IL-22 (Kidd, 2003; Steinman, 2007).

Th2-type cytokines such as IL-4 and IL-5 influence a wide range of events associated with allergic inflammation. IL-4 stimulates the

* Corresponding author. Tel./fax: +81 76 234 4407.
E-mail address: tyokoi@kenroku.kanazawa-u.ac.jp (T. Yokoi).

0378-4274/$ – see front matter © 2010 Elsevier Ireland Ltd. All rights reserved.
doi:10.1016/j.toxlet.2010.11.006

production of IgE and promotes the development of mast cells. IL-5 is involved in the development of eosinophils (Kay, 2001). In concanavalin (Con) A-mediated hepatitis, a widely accepted mouse model for studying T cell-mediated liver injury, IL-4 stimulates the secretion of Eotaxin-1 and enhances IL-5 production resulting in the attraction of neutrophils and eosinophils into the liver which leads to hepatitis (Jaruga et al., 2003).

Prostaglandin D_2 (PGD_2) is implicated in various allergic inflammatory diseases, such as atopic dermatitis, allergic asthma, and airway inflammation. It has been reported that PGD_2 has protective roles in acetaminophen-induced liver injury and 15-deoxy PGJ_2, which is metabolite of PGD_2, enhances allyl alcohol-induced hepatotoxicity (Reilly et al., 2001; Maddox et al., 2004). PGD_2 elicits biological responses by activating two receptors, the D-prostanoid receptor (DP) and the chemoattractant receptor homologous-molecule expressed on T-helper-type-2 cells (CRTh2), which are linked to different signaling pathways. CRTh2 expresses in eosinophils, basophils, and Th2 cells, but not in hepatocytes or endothelial cells. The decrease in cAMP levels and mobilization of intracellular Ca^{2+} mediated by CRTh2 activation leads to the chemotaxis of Th2 lymphocytes, eosinophils, and monocytes. 13,14-Dihydro-15-keto-prostaglandin D_2 (DK-PGD_2) is a selective CRTh2 agonist that does not activate DP, as reviewed by Kostenis and Ulven (2006). CRTh2 activation plays a significant role in Th2-dependent neutrophil inflammation (Takeshita et al., 2004). In this study, we found that dicloxacillin-induced liver injury is mediated by IL-4 and exacerbated by DK-PGD_2 in mice.

2. Materials and methods

2.1. Chemicals

Dicloxacillin was purchased from Sigma (St. Louis, MO). RNAiso was from Nippon Gene (Tokyo, Japan). Fuji DRI-CHEM slides of GPT/ALT-PIII and TBIL-PIII to measure alanine aminotransferase (ALT) and total-bilirubin (T-Bil), respectively, were from Fujifilm (Tokyo, Japan). ReverTra Ace was from Toyobo (Tokyo, Japan). Random hexamer and SYBR Premix Ex Taq were from Takara (Osaka, Japan). All primers were commercially synthesized at Hokkaido System Sciences (Sapporo, Japan). 13,14-Dihydro-15-keto-prostaglandin D_2 (DK-PGD_2) was purchased from Cayman Chemical (Denver, CO). Recombinant mouse IL-4 (rIL-4) was from Endogen (Cambridge, MA). Rabbit polyclonal antibody against myeloperoxidase (MPO) was from DAKO (Carpinteria, CA). Monoclonal anti-mouse IL-4 antibody was from U-Cytech Bioscienses (Utrecht, Netherlands). Monoclonal rat IgG2a isotype, used as a control, from R&D Systems (Abingdon, UK). A Ready-SET-GO! Mouse Interleukin-4 (IL-4) enzyme-linked immunosorbent assay (ELISA) kit was from eBioscience (San Diego, CA). Other chemicals were of analytical or the highest grade commercially available.

2.2. Mouse models of dicloxacillin-induced liver injury

Female BALB/cCrSlc mice (6 weeks old) were obtained from SLC Japan (Hamamatsu, Japan). Mice were housed in a controlled environment (temperature 25 ± 1 °C, humidity 50 ± 10%, and 12 h light/12 h dark cycle) in the institutional animal facility with access to food and water *ad libitum*. Animals were acclimatized before use for the experiments. Mice were administered intraperitoneally (i.p.) dicloxacillin (600 mg/kg, dissolved in saline) in a non-fasting condition. Six hours after dicloxacillin administration, the animals were sacrificed and the blood was collected from inferior vena cava, and liver from the biggest lobe. For measurement of the plasma IL-4 level, mice were sacrificed at 6 h after the dicloxacillin administration. A portion of each excised liver was fixed in 10% formalin neutral buffer solution and used for immunohistochemical staining. The degree of liver injury was assessed by hematoxylin–eosin (H&E) staining. Infiltration of mononuclear cells was assessed by immunostaining for MPO. Rabbit polyclonal antibody against MPO was used for immunohistochemical staining of liver as previously described (Kumada et al., 2004). Animal maintenance and treatment were conducted in accordance with the National Institutes of Health Guide for Animal Welfare of Japan, as approved by the Institutional Animal Care and Use Committee of Kanazawa University, Japan.

2.3. Real-time reverse transcription (RT)-PCR

RNA from the mouse liver was isolated using RNAiso according to the manufacturer's instructions. T-bet, GATA-3, ROR-γt, IFN-γ, IL-5, STAT1, STAT3, STAT6, Eotaxin-1, monocyte chemoattractant protein-1 (MCP-1) and macrophage inflammatory protein-2 (MIP-2) were quantified by real-time RT-PCR. The primer sequences used in this study are shown in Table 1. For the RT-process, total RNA (10 μg) and 150 ng random hexamer were mixed and incubated at 70 °C for 10 min. RNA solution was added to a reaction mixture containing 100 units of ReverTra Ace, reaction buffer and 0.5 mM dNTPs in a final volume of 40 μl. The reaction mixture was incubated at 30 °C for 10 min, 42 °C for 1 h, and heated at 98 °C for 10 min to inactivate the enzyme. The real-time RT-PCR was performed using the Mx3000P instrument (Stratagene, La Jolla, CA). The PCR mixture contained 1 μl or 2 μl of template cDNA, SYBR Premix Ex Taq solution and 8 pmol of forward and reverse primers. Amplified products were monitored directly by measuring the increase of the dye intensity of the SYBR Green I (Molecular Probes, Eugene, OR).

Table 1
Sequences of primers used for real-time RT-PCR analyses.

Gene		Sequences
mIL-5	FP	5′-AAA GAG ACC TTG ACA CAG CTG-3′
	RP	5′-CCA CGG ACA GTT TGA TTC TTC-3′
mIFN-γ	FP	5′-GGC CAT CAG CAA CAT AAG C-3′
	RP	5′-TGG ACC ACT CGG ATG AGC TCA-3′
mGATA-3	FP	5′-GGA GGA CTT CCC CAA GAG CA-3′
	RP	5′-CAT GCT GGA AGG GTG GTG A-3′
mT-bet	FP	5′-CAA GTG GGT GCA GTG TGG AAA G-3′
	RP	5′-TGG AGA GAC TGC AGG ACG ATC-3′
mROR-γt	FP	5′-ACC TCC ACT GCC AGC TGT GTG CTG TC-3′
	RP	5′-TCA TTT CTG CAC TTC TGC ATG TAG ACT GTC CC-3′
mSTAT-6	FP	5′-ATC TTC AAC GAC AAC AGC CTC A-3′
	RP	5′-GGA GAA GGC TAG TGA CAT ATT G-3′
mSTAT-1	FP	5′-GTT TCA GCT CTG CTC CAT AC-3′
	RP	5′-CTG CTG AAG CTC GAA CCA C-3′
mSTAT-3	FP	5′-TGC AGA GCA GGT ATC TTG AG-3′
	RP	5′-TGC TGC TTC TCT GTC ACT AC-3′
mEotaxin-1	FP	5′-TCC ACA GCG CTT CTA TTC CT-3′
	RP	5′-CTA TGG CTT TCA GGG TGC AT-3′
mMCP-1	FP	5′-TGT CAT GCT TCT GGG CCT G-3′
	RP	5′-CCT CTC TCT TGA GCT TGG TG-3′
mMIP-2	FP	5′-AAG TTT GCC TTG ACC CTG AAG-3′
	RP	5′-ATC AGG TAC GAT CCA GGC TTC-3′
mGAPDH	FP	5′-AAA TGG GGT GAG GCC GGT-3′
	RP	5′-ATT GCT GAC AAT CTT GAG TGA-3′

FP: forward primer, RP: reverse primer.

2.4. Administration of recombinant mouse IL-4 (rIL-4) or anti-mouse IL-4 antibody

One hour after dicloxacillin administration, rIL-4 was intraperitoneally administered (0.5 or 2.0 μg of rIL-4 in 0.2 ml of sterile PBS containing 0.5% BSA) in a non-fasting condition. As a control, vehicle was administered. In the neutralization study, mice were administered anti-mouse IL-4 antibody intraperitoneally (100 μg of anti-mouse IL-4 antibody in 0.2 ml of sterile PBS), 1 h before dicloxacillin administration. As a control, rat IgG2a was administered (100 μg of rat IgG2a in 0.2 ml of sterile PBS).

2.5. Treatment of DK-PGD_2

One hour after dicloxacillin administration, mice were administered with DK-PGD_2 intraperitoneally (10 μg/mouse, dissolved in 200 μl of PBS) in a non-fasting condition. As a control, vehicle was administered.

2.6. Measurement of plasma IL-4 level

Plasma IL-4 level was measured by enzyme-linked immunosorbent assay (ELISA) using a Ready-SET-GO! Mouse IL-4 kit according to the manufacturer's instructions.

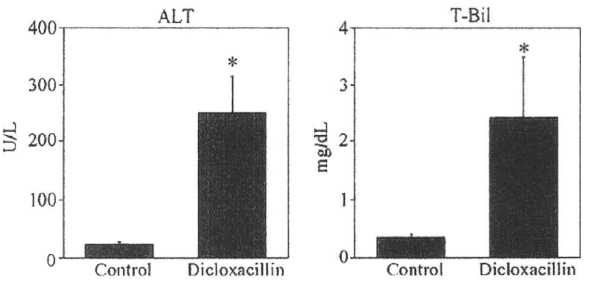

Fig. 1. Plasma ALT and T-Bil levels in dicloxacillin-administered mice. Mice were administered dicloxacillin (600 mg/kg, i.p.), and plasma for ALT and T-Bil were collected 6 h after the administration. Data are mean ± SD ($n = 4$; control, 5; dicloxacillin). Significantly different from saline-administered control mice ($^*p < 0.05$).

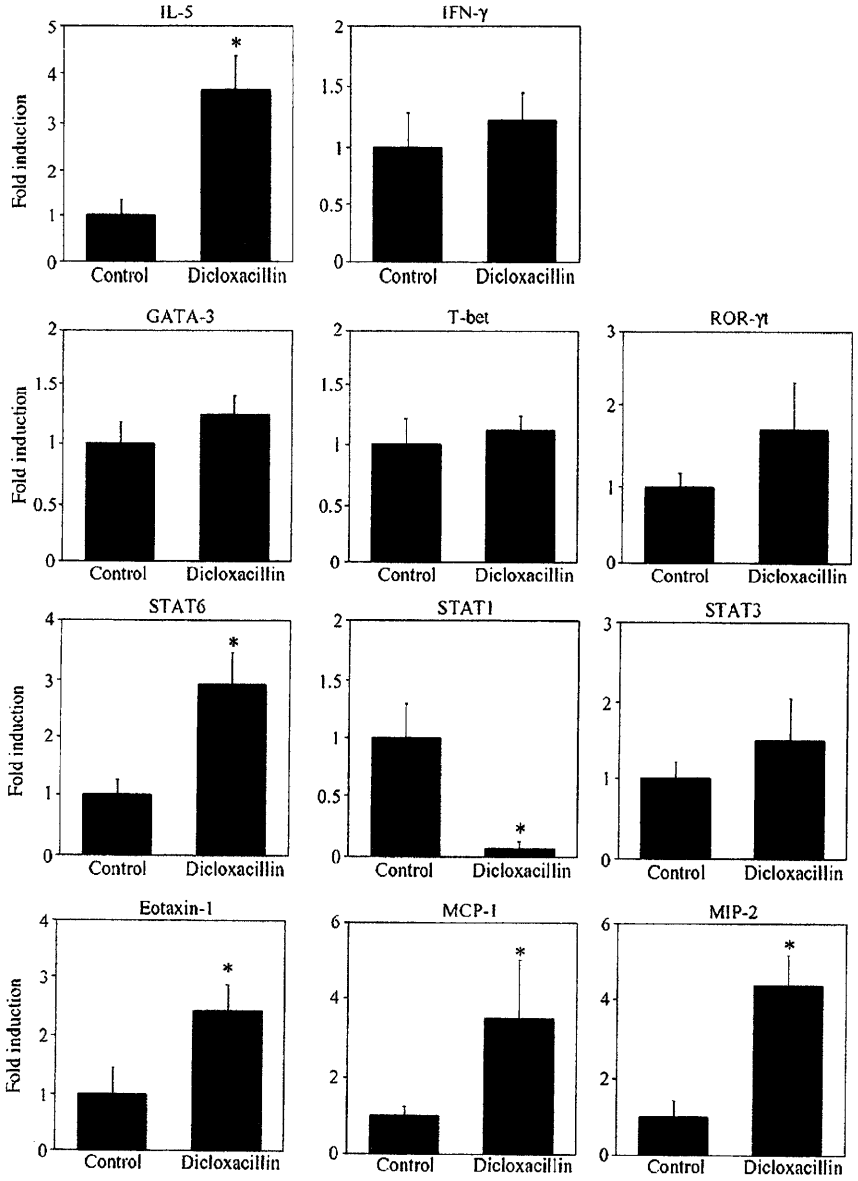

Fig. 2. Hepatic mRNA levels of transcription factors, cytokines and chemokines in dicloxacillin-administered mice. Mice were administered dicloxacillin (600 mg/kg, i.p.), and the hepatic IL-5, IFN-γ, GATA-3, T-bet, ROR-γt, STAT6, STAT1, STAT3, Eotaxin-1, MCP-1, and MIP-2 mRNA levels were measured by real-time RT-PCR 6 h after the administration. Data are mean ± SD ($n = 4$; control, 5; dicloxacillin). Significantly different from saline-administered control mice ($^*p < 0.05$).

2.7. Statistical analysis

Data are presented as mean ± SD. Statistical analyses between multiple groups were performed using one-way analysis of variance (ANOVA), followed by Tukey's post hoc test, and comparisons between two groups were carried out using two-tailed Student's t test in mRNA and plasma IL-4 level. In ALT and T-Bil levels, non-parametric statistical analysis was conducted using the Mann–Whitney U test and Kruskal–Wallis test. $p < 0.05$ was considered statistically significant.

3. Results

3.1. Increase of plasma ALT and T-Bil levels in dicloxacillin-administrated mice

Female BALB/c mice were administered dicloxacillin at a dose of 600 mg/kg. Plasma ALT and T-Bil (Fig. 1) were significantly increased 6 h after dicloxacillin administration. The administration of dicloxacillin at a dose of 400 mg/kg did not affect on the ALT and T-Bil levels (data not shown).

3.2. Expression of transcription factor, cytokine, and chemokine genes in dicloxacillin-administered mouse liver

To investigate the involvement of immunological factors in the dicloxacillin hepatotoxicity, hepatic mRNA levels of IL-5, IFN-γ, GATA-3, T-bet, ROR-γt, STAT6, STAT1, STAT3, Eotaxin-1, MCP-1, and MIP-2 were measured by real-time RT-PCR. IL-5, STAT6, Eotaxin-1, MCP-1, and MIP-2 expressions were significantly increased in dicloxacillin-administered mice compared with the control mice, whereas STAT1 expression was significantly decreased. Furthermore, T-bet, GATA-3, ROR-γt, IFN-γ, and STAT3 expressions were

not changed (Fig. 2). These results suggested that Th2-related factors, such as IL-5, STAT6, and Eotaxin-1, were involved in the dicloxacillin-induced liver injury.

3.3. Plasma IL-4 level in dicloxacillin-administered mouse liver

IL-4 is a cytokine which activates STAT6 (Nelms et al., 1999), and is a major factor in Con A-induced hepatitis (Jaruga et al., 2003). To investigate whether IL-4 was involved in the dicloxacillin-induced liver injury, we measured plasma IL-4 in dicloxacillin-administered mice (Fig. 3). Plasma IL-4 level was significantly increased in dicloxacillin-administered group compared with the control mice.

3.4. Exacerbation of hepatotoxic effect by rIL-4 administration, and amelioration by anti-IL-4 antibody administration

To further investigate whether IL-4 was involved in the dicloxacillin-induced liver injury, we performed rIL-4 administration and IL-4 neutralization studies (Fig. 4). In the dicloxacillin/rIL-4 cotreatment study, the plasma ALT level was increased significantly and dose-dependently in mice coadministered 2.0 μg/mouse

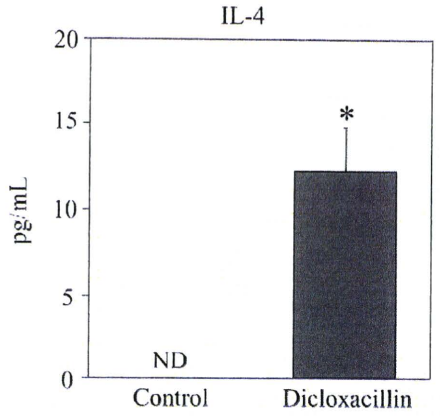

Fig. 3. Plasma IL-4 level in dicloxacillin-administered mice. Mice were administered dicloxacillin (600 mg/kg, i.p.), and plasma was collected 6 h after the administration. Data are mean ± SD ($n = 4$; control, 5; dicloxacillin). Significantly different from saline-administered control mice ($^{*}p < 0.05$).

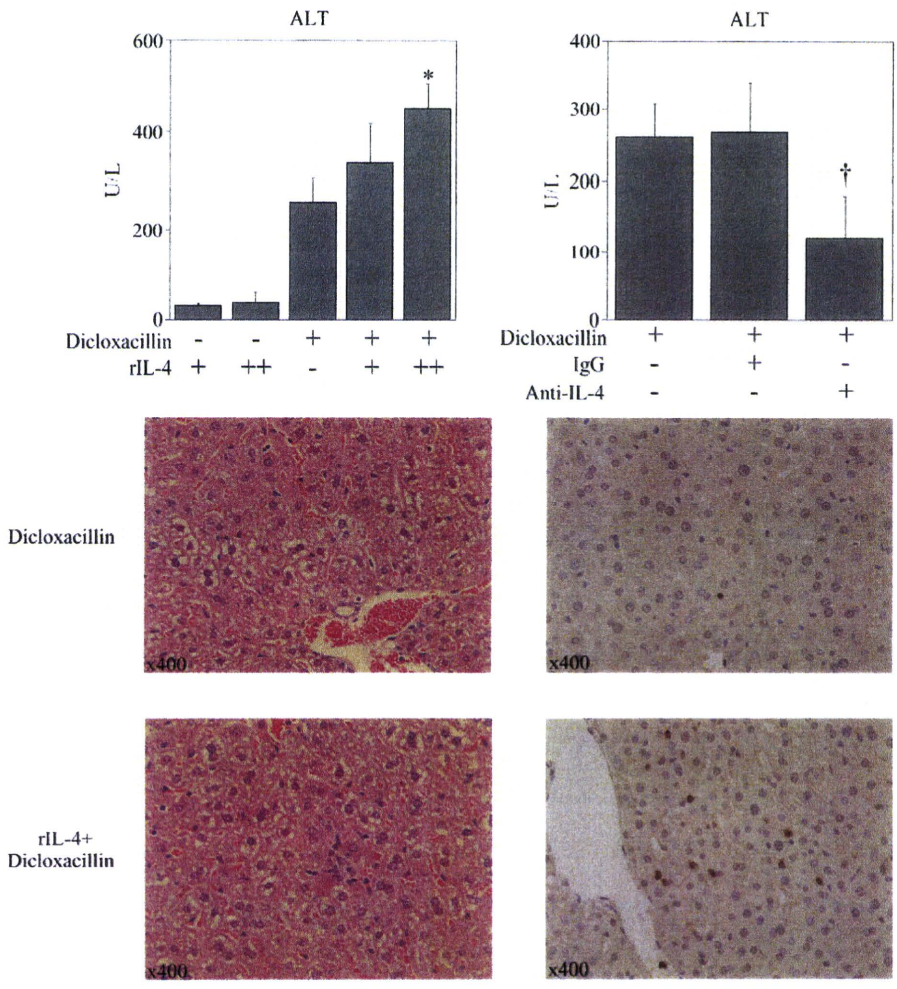

Fig. 4. Effects of recombinant mouse IL-4 (rIL-4) or anti-mouse IL-4 antibody administration on plasma ALT in dicloxacillin-administered mice. Mice were administered dicloxacillin (600 mg/kg, i.p.) and the plasma ALT was measured 6 h after the administration. In the rIL-4 administration study, rIL-4 (0.5 or 2.0 μg/mouse indicated + or ++, respectively) was administered, 1 h after dicloxacillin administration. In the IL-4 neutralization study, anti-mouse IL-4 antibody (0.1 mg/mouse, i.p.) was administered, 1 h before dicloxacillin administration. Liver specimens were prepared 6 h after the dicloxacillin administration. Liver tissue sections were stained with H&E (left photos) or immunostained with anti-MPO antibody (right photos). Data are mean ± SD ($n = 4$–5). Significantly different from dicloxacillin-administered group ($^{*}p < 0.05$); significantly different from dicloxacillin-plus control IgG2a administered group ($^{\dagger}p < 0.05$).

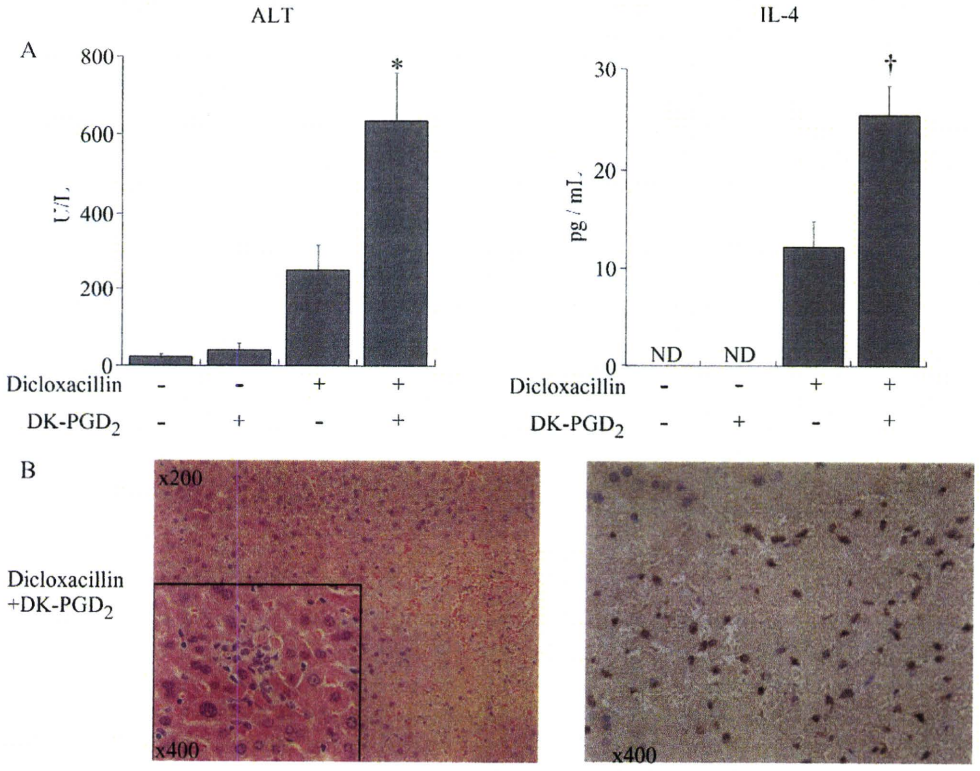

Fig. 5. Effects of DK-PGD_2 treatment on dicloxacillin-induced liver injury in mice. Mice were administered dicloxacillin (600 mg/kg, i.p.), and the plasma ALT and IL-4 levels were measured 6 h after the administration (A). One hour after dicloxacillin administration, DK-PGD_2 (10 μg/mouse, i.p.) was administered. Liver specimens (B) were prepared 6 h after the dicloxacillin administration. Liver tissue sections were stained with H&E (left photo) or immunostained with anti-MPO antibody (right photo). Data are mean ± SD (dicloxacillin and/or DK-PGD_2 administered). Significantly different from saline-administered group ($^*p < 0.05$); significantly different from dicloxacillin-administered mice ($^\dagger p < 0.05$).

rIL-4 compared with only dicloxacillin-administered mice. However, rIL-4 alone did not induce liver injury in mice. In the H&E staining, infiltration of mononuclear cells into the hepatocytes was observed in the dicloxacillin/rIL-4-coadministered group but not in the dicloxacillin-administered group. In anti-MPO staining, the numbers of MPO-positive mononuclear cells were increased in the dicloxacillin/rIL-4-coadministered group compared with dicloxacillin-administered group. In the neutralization study, the i.p. administration of anti-mouse IL-4 antibody significantly reduced the plasma ALT, but rat IgG2 treatment demonstrated no effect on the dicloxacillin-induced liver injury.

3.5. *Effects of DK-PGD_2 treatment*

We investigated the effects of DK-PGD_2, a selective CRTh2 agonist, on dicloxacillin-induced liver injury. Administration of DK-PGD_2 alone did not increase the plasma ALT and IL-4 levels, and DK-PGD_2 alone at a higher dose (50 μg/mouse, i.p.) did not increase ALT level (data not shown). The plasma ALT and IL-4 levels were significantly increased in the dicloxacillin/DK-PGD_2-coadministered group compared with the saline-administered group (Fig. 5A). In the histopathological study, spotty necrosis and infiltration of MPO-positive mononuclear cells were observed in the dicloxacillin/DK-PGD_2-coadministered group, but not in the dicloxacillin-administered group (Fig. 5B).

3.6. *Effects on liver mRNA expressions in DK-PGD_2 administered mice*

To evaluate the underlying mechanisms responsible for the increased susceptibility of DK-PGD_2 administered mice to dicloxacillin-induced liver injury, the mRNA expression levels were assessed. The hepatic mRNA levels of GATA-3, Eotaxin-1, MCP-1 and MIP-2 were significantly increased compared with the dicloxacillin-administered mice (Fig. 6). Especially, MIP-2 mRNA was markedly increased. In contrast, IFN-γ, IL-5, ROR-γt, STAT3, and STAT6 were not changed, and T-bet and STAT1 were significantly decreased (data not shown).

4. Discussion

Adverse drug reactions to antibiotics are variable, but severe liver injury is rarely reported (Bjornsson and Olsson, 2005) and the mechanism of antibiotic-induced liver injury remains to be clarified. Dicloxacillin, penicillinase-sensitive penicillin, rarely causes liver injury and there is some evidence for an immunoallergic idiosyncratic reaction (Olsson et al., 1992). In the present study, dicloxacillin-induced liver injury was investigated in mice. Firstly, we investigated the effects of dicloxacillin administration on ALT and T-Bil in normal female BALB/c mice (Fig. 1). BALB/c mice were previously used as a model for halothane-induce liver injury, which is mediated by immunological factors (Kobayashi et al., 2009). The ALT increase induced by dicloxacillin was attenuated after 24 h, compared with those after 6 h (data not shown). This is the first mice model to study dicloxacillin-induced liver injury. Flucloxacillin, which is structural homologue of dicloxacillin, has a higher incidence of liver injury than dicloxacillin (Bjornsson and Olsson, 2005; Olsson et al., 1992) and it has been recently reported that HLA allele is a major biomarker of DILI due to flucloxacillin (Daly et al., 2009), suggested that immune responses are mainly involved in flucloxacillin-induced liver injury. However, the mechanisms are unclear and there is no mouse model, we would like

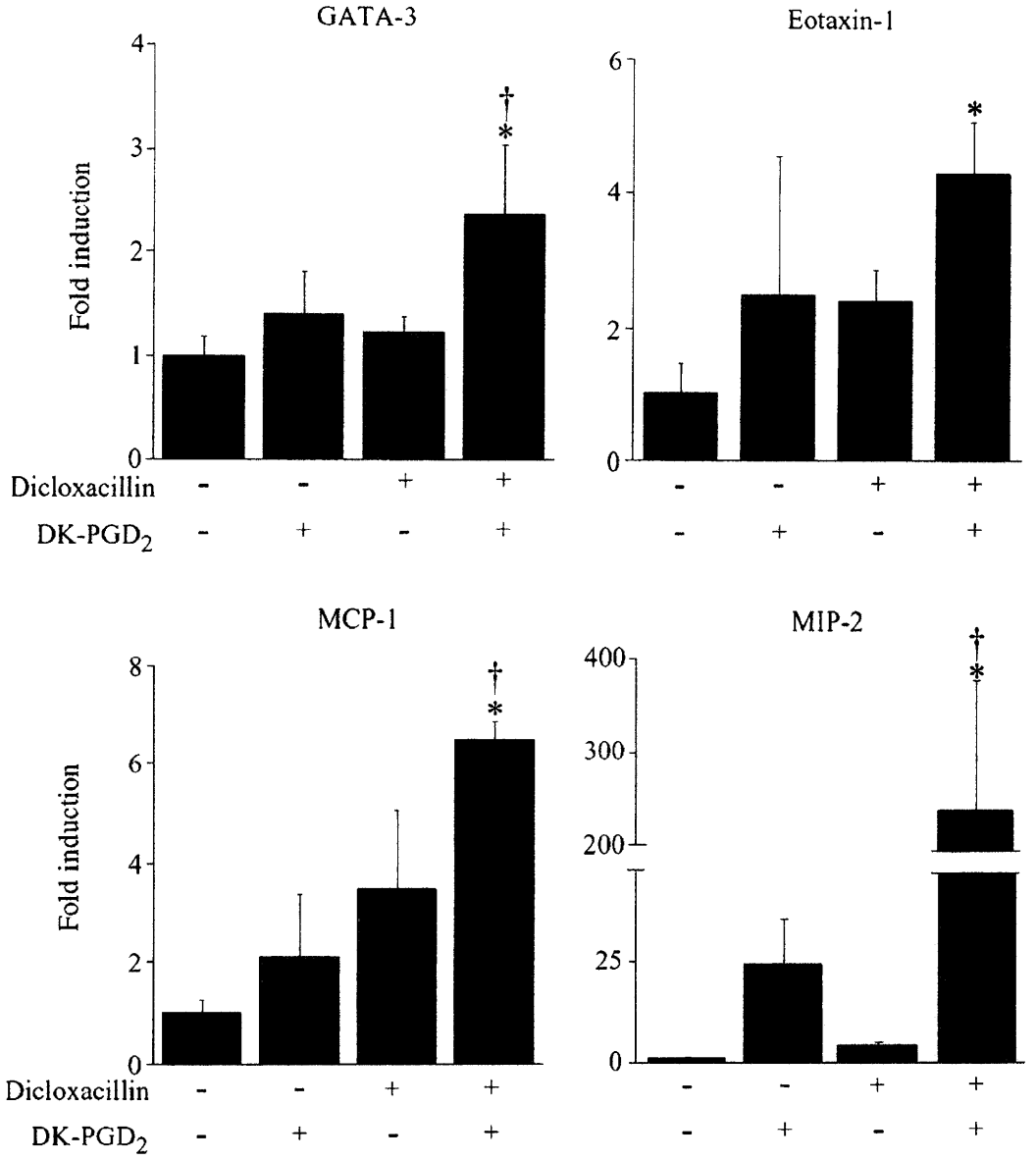

Fig. 6. Effects of DK-PGD_2 treatment on hepatic mRNA levels of transcription factor and chemokines in dicloxacillin-administered mice. Mice were administered dicloxacillin (600 mg/kg, i.p.). One hour after dicloxacillin administration, DK-PGD_2 (10 μg/mouse, i.p.) was administered. GATA-3, Eotaxin-1, MCP-1 and MIP-2 liver mRNA levels were measured by real time RT-PCR 6 h after the administration. Data are mean ± SD ($n = 4$; non-treatment, 5; dicloxacillin and/or DK-PGD_2 administered). Significantly different from saline-administered control mice ($^*p < 0.05$); significantly different from dicloxacillin-administered mice ($^\dagger p < 0.05$).

to investigate whether the mechanisms of liver injury due to flucloxacillin is similar to those of dicloxacillin.

In this study, a relationship between dicloxacillin-induced liver injury and immunological factors was demonstrated (Figs. 2 and 3). The administration of dicloxacillin significantly increased the expression of hepatic IL-5, STAT6, and Eotaxin-1 mRNA, whereas it decreased STAT1 mRNA. Plasma IL-4 was induced in dicloxacillin-administered mice. These results suggest that Th2-mediated factors could be involved in dicloxacillin-induced liver injury. It has been reported that IL-4 activates STAT6 which induces IL-5 and Eotaxins-1 (Jaruga et al., 2003), and induces SOCS1 and SOCS3 which inhibit the STAT1 activity (Palmer and Restifo, 2009). The mRNA expressions of chemokines such as MCP-1 and MIP-2 were significantly increased in dicloxacillin-administered mice. MCP-1 is increased in acetaminophen-induced liver injury (Dambach et al., 2006), and MIP-2 induces neutrophil recruitment and is markedly increased in halothane-induced liver injury (Biedermann et al., 2000; Kobayashi et al., 2009). Eotaxin-1 and IL-5 are involved in allergic inflammation (Kay, 2001). These chemokines might be involved in the dicloxacillin-induced liver injury.

We demonstrated that rIL-4 exacerbated the dicloxacillin-induced liver injury, and neutralization of IL-4 significantly inhibited the increase of the plasma ALT level (Fig. 4). In liver injury, IL-4, a multifunctional Th2 cytokine, plays a protective role in ischemia/reperfusion-induced liver injury. In addition, IL-4 plays a pivotal role in Con A-induced liver injury (Kato et al., 2000; Jaruga et al., 2003), and promotes hapten-induced pro-inflammatory responses in trifluoroacetyl chloride-induced liver injury (Njoku et al., 2009). Elevated IL-4 has been reported in human liver diseases such as chronic hepatitis C (Spanakis et al., 2002) and

primary biliary cirrhosis (Harada et al., 1997). In this study, IL-4 was demonstrated to be involved in the dicloxacillin-induced liver injury.

CRTh2, one of the PGD_2 receptors, plays a major role in atopic dermatitis, allergic asthma, and airway inflammation, and it was demonstrated that CRTh2 is responsible for PGD_2 chemotaxis of Th2 cells, eosinophils, basophils, and monocytes (Kostenis and Ulven, 2006). DK-PGD_2 is a CRTh2 selective agonist that enhances Th2-type inflammation (Spik et al., 2005). In this study, Th2-mediated immune responses were suggested to be involved in the dicloxacillin-induced liver injury, thus we hypothesized that DK-PGD_2 may exacerbate liver injury. The plasma ALT level was significantly increased in the dicloxacillin/DK-PGD_2-coadministered group (Fig. 5). DK-PGD_2 enhances the chemotactic responsiveness to other chemoattractants, as well as degranulation (Kostenis and Ulven, 2006). Therefore, it was conceivable that a higher ALT level would be observed in the dicloxacillin/DK-PGD_2-coadministered group than in the rIL-4/dicloxacillin-coadministered group (Figs. 4 and 5). The hepatic GATA-3 mRNA level was significantly increased in the dicloxacillin/DK-PGD_2-coadministered group suggesting an increase in Th2-mediated factors in the liver, followed by an increase in the plasma IL-4 level (Nelms et al., 1999). Hepatic mRNA levels of Eotaxin-1, MCP-1, and MIP-2 levels were significantly increased in the dicloxacillin/DK-PGD_2-coadministered group (Fig. 6). These chemokines induce the infiltration of neutrophils followed by necrosis. Especially, MIP-2 mRNA was markedly increased, since CRTh2 activation induces MIP-2 secretion (Takeshita et al., 2004). In this study, we demonstrated that DK-PGD_2 exacerbates dicloxacillin-induced liver injury due to induction of IL-4 and MIP-2, followed by the activation of Th2 cells and other immune cells.

Although the mechanisms of DILI are still unclear due to the lack of proper animal models, LPS-treated rodents become sensitive to human hepatotoxic drugs, such as sulindac, diclofenac, chlorpromazine, and trovafloxacin (Zou et al., 2009; Shaw et al., 2009). Cytokines such as TNF-α, IL-1, IL-6, and IFN-γ are upregulated after the activation of Toll-like receptor 4 by LPS (Gaestel et al., 2009; Shaw et al., 2009), however the involvement of Th2 factors in drug-induced liver injury in LPS-administered rodents was never reported. Enhanced responsiveness with DK-PGD_2 could be a novel method in drug development to detect human hepatotoxic drugs that involve Th2-specific factors.

In conclusion, we reported that Th2 immune factors, such as IL-4, IL-5, and Eotaxin-1, were involved in drug-induced liver injury in mice, and DK-PGD_2 exacerbates dicloxacillin-induced liver injury via Th2 cytokines and chemokines. The present study provides new insight into the mechanisms of drug-induced liver injury.

Funding

Health and Labor Sciences Research Grants from the Ministry of Health, Labor and Welfare of Japan (H20-BIO-G001).

Conflict of interest

None of the authors has any conflicts of interest related to this manuscript.

Acknowledgement

We thank Mr. Brent Bell for reviewing the manuscript.

References

Biedermann, B.T., Knelling, M., Mailhammer, R., Maier, K., Sander, C.A., Kollias, G., Kunkel, S.L., Hultner, L., Rocken, M., 2000. Mast cell control neutrophil recruitment during T cell-mediated delayed hypersensitivity reactions through tumor necrosis factor and macrophage inflammatory protein 2. J. Exp. Med. 192, 1441–1451.

Bjornsson, E., Olsson, R., 2005. Outcome and prognostic markers in severe drug-induced liver disease. Hepatology 42, 481–489.

Daly, A.K., Donaldson, P.T., Bhatnagar, P., et al., 2009. HLA-B*5701 genotype is a major determinant of drug-induced liver injury due to flucloxacillin. Nat. Genet. 41, 816–819.

Dambach, D.M., Durham, S.K., Laskin, J.D., Laskin, D.L., 2006. Distinct roles of NF-κB p50 in the regulation of acetaminophen-induced inflammatory mediator production and hepatotoxicity. Toxicol. Appl. Pharmacol. 211, 157–165.

Gaestel, M., Kotlyarov, A., Kracht, M., 2009. Targeting innate immunity protein kinase signaling in inflammation. Nat. Rev. Drug. Discov. 8, 480–497.

Harada, K., Water, J.V., Leung, P.S.C., Coppel, R.L., Ansari, A., Nakanuma, Y., Gershwin, M.E., 1997. *In situ* nucleic acid hybridization of cytokines in primary biliary cirrhosis: predominance of the Th1 subset. Hepatology 25, 791–796.

Heneghan, M.A., McFarlane, I.G., 2002. Current and novel immunosuppressive therapy for autoimmune hepatitis. Hepatology 35, 7–13.

Holt, M.P., Ju, C., 2006. Mechanisms of drug-induced liver injury. AAPS J. 8, 48–54.

Jaruga, B., Hong, F., Sun, R., Radaeva, S., Gao, B., 2003. Crucial role of IL-4/STAT6 in T cell-mediated hepatitis: up-regulating eotaxins and IL-5 and recruiting leukocytes. J. Immunol. 171, 3233–3244.

Kato, A., Yoshidome, H., Edwards, M.J., Lentsch, A.B., 2000. Reduced hepatic ischemia/reperfusion injury by IL-4: potential anti-inflammatory role of STAT6. Inflamm. Res. 49, 275–279.

Kay, A.B., 2001. Allergy and allergic diseases. N. Engl. J. Med. 344, 30–37.

Kidd, P., 2003. Th1/Th2 balance: the hypothesis, its limitations, and implications for health and disease. Altern. Med. Rev. 8, 223–246.

Kita, H., Macky, I.R., Van, D.W.J., Gershwin, M.E., 2001. The lymphoid liver: considerations on pathways to autoimmune injury. Gastroenterology 120, 1485–1501.

Kobayashi, E., Kobayashi, M., Tsuneyama, K., Fukami, T., Nakajima, M., Yokoi, T., 2009. Halothane-induced liver injury is mediated by interleukin-17 in mice. Toxicol. Sci. 111, 302–310.

Kostenis, E., Ulven, T., 2006. Emerging roles of DP and CRTh2 in allergic inflammation. Trends Mol. Med. 12, 148–158.

Kumada, T., Tsuneyama, K., Hatta, H., Ishizawa, S., Takano, Y., 2004. Improved 1-h rapid immunostaining method using intermittent microwave irradiation: practicability based on 5 years application in Toyama Medical and Pharmaceutical University Hospital. Mod. Pathol. 17, 1141–1149.

Leonard, W.J., O'Shea, J.J., 1998. Jaks and STATs: biological implications. Annu. Rev. Immunol. 16, 293–322.

Maddox, J.F., Domzalski, A.C., Roth, R.A., Ganey, P.E., 2004. 15-Deoxy prostaglandin J_2 enhances allyl alcohol-induced toxicity in rat hepatocytes. Toxicol. Sci. 77, 290–298.

Nelms, K., Keegan, A.D., Zamorano, J., Ryan, J.J., Paul, W.E., 1999. The IL-4 receptor: signaling mechanisms biologic functions. Annu. Rev. Immunol. 17, 701–738.

Njoku, D.B., Li, Z., Washington, N.D., Mellerson, J.L., Talor, M.V., Sharma, R., Rose, N.R., 2009. Suppressive and pro-inflammatory roles for IL-4 in the pathogenesis of experimental drug-induced liver injury. Eur. J. Immunol. 39, 1652–1663.

Olsson, R., Wiholm, B.E., Sand, C., Zettergren, L., Hultcrantz, R., Myehed, M., 1992. Liver damage from flucloxacillin, cloxacillin, dicloxacillin. J. Hepatol. 15, 154–161.

Palmer, C.D., Restifo, P.N., 2009. Suppressors of cytokine signaling (SOCS) in T cell differentiation, maturation, and function. Trends Immunol. 30, 592–602.

Reilly, T.P., Brady, J.N., Marchick, M.R., Bourdi, M., George, J.W., Radonovich, M.F., Pise-Masison, C.A., Pohl, L.R., 2001. A protective role for cyclooxygenase-2 in drug-induced liver injury in mice. Chem. Res. Toxicol. 14, 1620–1628.

Shaw, P.J., Ditewig, A.C., Waring, J.F., Liguori, M.J., Blomme, E.A., Ganey, P.E., Roth, R.A., 2009. Coexposure of mice to trovafloxacin and lipopolysaccharide, a model of idiosyncratic hepatotoxicity, results in a unique gene expression profile and interferon gamma-dependent liver injury. Toxicol. Sci. 107, 270–280.

Spanakis, N.E., Garinis, G.A., Alexopoulos, E.C., Patrinos, G.P., Menounos, P.G., Sklavounou, A., Manolis, N.E., Gorgoulis, V.G., Valis, D., 2002. Cytokines serum levels in patients with chronic HCV infection. J. Clin. Lab. Anal. 16, 40–46.

Spik, I., Brenuchon, C., Angeli, V., Staumont, D., Fleury, S., Capron, M., Trottein, F., Dombrowicz, D., 2005. Activation of the prostaglandin D_2 receptor DP2/CRTH2 increases allergic inflammation in mouse. J. Immunol. 174, 3703–3708.

Stein, G.E., 2005. Safety of newer parenteral antibiotics. Clin. Infect. Dis. 41, 293–302.

Steinman, L., 2007. A brief history of Th17, the first major revision in the Th1/Th2 hypothesis if T cell-mediated tissue damage. Nat. Rev. Med. 13, 139–145.

Takeshita, K., Yamasaki, T., Nagano, K., Sugimoto, H., Shichijo, M., Gantner, F., Bacon, B.K., 2004. CRTH2 is a prominent effector in contact hypersensitivity-induced neutrophil inflammation. Int. Immunol. 16, 947–959.

Zou, W., Devi, S.S., Sparkenbaugh, E., Younis, H.S., Roth, R.A., Ganey, P.E., 2009. Hepatotoxic interaction of sulindac with lipopolysaccharide: role of the hemostatic system. Toxicol. Sci. 108, 184–193.